REPORT DOCUMENTATION PAGE

Form Approved
OMB No. 0704-0188

Public reporting burden for this collection of information is estimated to average 1 hour per response, including the time for reviewing instructions, searching existing data sources, gathering and maintaining the data needed, and completing and reviewing the collection of information. Send comments regarding this burden estimate or any other aspect of this collection of information, including suggestions for reducing this burden, to Washington Headquarters Services, Directorate for Information Operations and Reports, 1215 Jefferson Davis Highway, Suite 1204, Arlington, VA 22202-4302, and to the Office of Management and Budget, Paperwork Reduction Project (0704-0188), Washington, DC 20503.

1. AGENCY USE ONLY (Leave blank)	2. REPORT DATE	3. REPORT TYPE AND DATES COVERED
	May 1, 1997	final

4. TITLE AND SUBTITLE

DIESEL ENGINE COLD-STARTING STUDIES: OPTICALLY ACESSIBLE ENGINE EXPERIMENTS AND MODELING

5. FUNDING NUMBERS

DAAL03-92-G-0168

6. AUTHOR(S)

Naeim A. Henein and Ming-Chia Lai

7. PERFORMING ORGANIZATION NAME(S) AND ADDRESS(ES)

CENTER FOR AUTOMOTIVE RESEARCH
WAYNE STATE UNIVERSITY
DETORIT, MI 48202

8. PERFORMING ORGANIZATION REPORT NUMBER

9. SPONSORING/MONITORING AGENCY NAME(S) AND ADDRESS(ES)

U.S. Army Research Office
P.O. Box 12211
Research Triangle Park, NC 27709-2211

10. SPONSORING/MONITORING AGENCY REPORT NUMBER

ARO 29302.1-EG

11. SUPPLEMENTARY NOTES

The views, opinions and/or findings contained in this report are those of the author(s) and should not be construed as an official Department of the Army position, policy, or decision, unless so designated by other documentation.

12a. DISTRIBUTION/AVAILABILITY STATEMENT

Approved for public release; distribution unlimited.

12b. DISTRIBUTION CODE

13. ABSTRACT *(Maximum 200 words)*

An experimental and numerical study was carried out to simulate the diesel spray breakup, vaporization, ignition, and combustion during cold starting conditions. This report summarizes the optical diagnostics and multi-dimensional computation results for two single-cylinder optically accessible engines. The results showed that optically accessible engines provide very useful information for studying the diesel cold starting conditions, which also provide a critical test for diesel combustion models. The pre-ignition chemistry showed great sensitivity to the compressed air temperature. KIVA with a modified shell model responds accordingly to the change of inlet air temperatures and fuel injection parameters. However, other submodels do not have enough sensitivity to simulate the starting of diesel engine without careful validation and further improvements. A method to compute the ignition delay in engines from data obtained in constant volume vessels was also developed. The method accounts for the effect of variations in charge pressure and temperature on the formation of the chain carriers from the combustible mixture during the ID period. A comparison is made between the computed ID and data obtained in a LABECO research engine under different ambient temperatures ranging from +20° to -10° C.

14. SUBJECT TERMS

Diesel Engine combustion, diesel engine cold starting, ignition delay optically accessible engine, laser diagnostics, KIVA, engine modeling,

15. NUMBER OF PAGES

16. PRICE CODE

17. SECURITY CLASSIFICATION OF REPORT	18. SECURITY CLASSIFICATION OF THIS PAGE	19. SECURITY CLASSIFICATION OF ABSTRACT	20. LIMITATION OF ABSTRACT
UNCLASSIFIED	UNCLASSIFIED	UNCLASSIFIED	UL

DTIC QUALITY INSPECTED 4

DIESEL ENGINE COLD-STARTING STUDIES: OPTICALLY ACESSIBLE ENGINE EXPERIMENTS AND MODELING

FINAL REPORT

Naeim A. Henein and Ming-Chia Lai

May 1, 1997

U. S. ARMY RESEARCH OFFICE

GRANT No. DAAL03-92-G-0168

CENTER FOR AUTOMOTIVE RESEARCH
WAYNE STATE UNIVERSITY
DETORIT, MI 48202

APPROVE FOR PUBLIC RELEASE;
DISTRIBUTION UNLIMITED

19971204 077

EXCUTATIVE SUMMARY

An experimental and numerical study was carried out to simulate the diesel spray breakup, vaporization, ignition, and combustion during cold starting conditions. This report contains two parts.

Part I summarizes the optical diagnostics and multi-dimensional computation results for two single-cylinder optically accessible engines. The results showed that optically accessible engines provide very useful information for studying the diesel cold starting conditions, which also provide a critical test for diesel combustion models. The pre-ignition chemistry showed great sensitivity to the compressed air temperature. KIVA with a modified shell model responds accordingly to the change of inlet air temperatures and fuel injection parameters. However, other submodels do not have enough sensitivity to simulate the starting of diesel engine without careful validation and further improvements.

Part II presents a method to compute the ignition delay in engines from data obtained in constant volume vessels. The method accounts for the effect of variations in charge pressure and temperature on the formation of the chain carriers from the combustible mixture during the ID period. A comparison is made between the computed ID and data obtained in a LABECO research engine under different ambient temperatures ranging from $+20^{\circ}$ to -10° C.

TABLE OF CONTENTS

LIST OF FIGURES

LIST OF TABLES

PART I: Diesel Cold-Starting Study using Optically Accessible Engines

ABSTRACT

An experimental and numerical study was carried out to simulate the diesel spray behavior during cold starting condition inside two single-cylinder optically accessible engines. One is an AVL single-cylinder research diesel engine converted for optical access; the other is a TACOM/LABECO engine retrofitted with mirror-coupled endoscope access. The first engine is suitable for sophisticated optical diagnostics but is constrained to limited consecutive fuel injections or firings. The second one is located inside a micro-processor controlled cold room; therefore it can be operated under a wide range of practical engine conditions and is ideal for cycle-to-cycle variation study.

The intake and blow-by flow rates are carefully measured in order to clearly define the operation condition. In addition to cylinder pressure measurement, the experiment used 16-mm high-speed movie photography to directly visualize the global structures of the sprays and ignition process. A photodiode was used to quantify the ignition and combustion event through the endoscope for the LABECO engine. Limited tests using two laser diagnostics techniques were also carried out on the AVL engine to help characterize the key physical processes involved in the fuel-air mixing. Planar laser-induced exciplex fluorescence was used to visualize the vaporizing diesel sprays; phase Doppler analyzer system was also employed to perform the simultaneous measurements of droplet size and velocity. A modified version of KIVA-II was

used to evaluate the blowby, spray and multistep pre-ignition kinetics models for the AVL engine data.

The results showed that optically accessible engines provide very useful information for studying the diesel cold starting conditions, which also provide a critical test for diesel combustion models. The pre-ignition chemistry showed great sensitivity to the compressed air temperature. KIVA with a modified shell model responds accordingly to the change of inlet air temperatures and fuel injection parameters. However, other submodels do not have enough sensitivity to simulate the starting of diesel engine without careful validation and further improvements. Blowby model is very critical for cold starting condition but current model underestimates the temperature effect. Widely used empirical correlations and breakup models tend to overpredict the penetration of the low pressure diesel spray typically observed during cold starting.

INTRODUCTION

The superior performance and efficiency of diesel engines, as compared to other types of combustion engines, make them the preferred power plant for many propulsion and power generation needs. The diesel's tolerance to fuel properties makes it most suitable for multi-fuel applications, with the potential for both reducing undesirable emissions and reliance of petroleum fuels. The cold startability of a diesel engine is a practical and important concern when operation under low ambient temperature conditions is required. It is also a very complicated problem and extremely sensitive to various engine parameters and operation conditions.

The diesel cold starting problem can be characterized as a situation where either the combustion event in the cylinder is present on one cycle and absent in subsequent cycles (the so-called borderline condition of starting) or not present at all in the limiting case. Combustion failure may be due to a lack of autoignition caused by very slow pre-ignition reactions and the failure to form autoignition in the fuel-spray-air mixture, or by the inability of the autoignition nuclei to burn the surrounding mixture. Misfiring occurs also, if the reactions do not produce enough net energy to overcome the frictional losses, and supply the energy needed to accelerate the engine to the idle speed.

Ignition delay has been related to engine starting very early (Austen and Lyn, 1959; Biddulph and Lyn, 1966), but many factors contribute to the autoignition process at cold starting. Low cranking speeds allow significant blowby to occur, which not only decreases the bulk temperature and pressure but also opposes the squish flow. Cold wall temperatures cause greater heat loss from the bulk gases to the chamber wall, further lowering their temperature and pressure. Low fuel injection pressures contribute to poor fuel delivery, inadequate spray penetration and poor atomization and fuel vaporization. As a result, the spray wall impingement phenomena are characterized by low impact velocity and droplet rebound. In summary, diesel cold starting is a very complicated issue, including the interactions of low temperature ignition and combustion process, crevice flow or blowby problem, instantaneous friction characteristics and cycle-to-cycle variations coupled with engine dynamics. Because of its sensitivity, it presents a greater challenge and more critical test, as compared to regular warm operations, for various physical and chemical models that are required to simulate engine processes and performances

In the past, most investigators have studied the diesel cold start problem in terms of description of the phenomena and development of devices (such as ignition aids: DeCarolis, et al., 1959; Kawamura and Yamamoto, 1983; Murayama et al., 1983; Dale et al., 1985) or techniques to solve the problem (such as compression ratio, combustion chamber design, injection timing, and injection rate shaping: Phatak and Nakamura, 1983; Ishida et al., 1986). There are also extensive studies in our laboratory on the effects of air temperature and pressure near the end of the compression process, the cetane number of the fuel, the instantaneous engine dynamics and friction, fuel injection, fuel-air mixing, and crevice flow (Henein et al., 1986-1992, Zahdeh et al., 1990, 1992). It has been found that combustion instability during diesel cold starting is not a random phenomenon, not fuel specific, and not engine specific (Bryzik and Henein, 1994). However, there is still very little research work that directly characterized the fuel injection and ignition process inside a diesel engine under cold starting conditions. For DI engines, the distribution of droplet sizes produced by the injector and the spatial distributions of liquid masses within its spray are of fundamental importance to fuel/air evaporation, mixing, and subsequent ignition and combustion. Therefore, applying optical diagnostics to optically-accessible engine (OAE) will provide direct visualization and measurement of the parameters involved in the cold starting process. For examples, Kobayashi et al. (1980) and Friz and Abata (1987) have applied high-speed movie photography to study diesel cold starting. Presently, multi-dimensional modeling has also been well-developed that most of the key processes in cold starting can be accounted for in the submodels. Gonzalez et al. (1991) were the first one to apply a modified KIVA-II program with improved spray breakup, blowby, wall impingement, and simplified one-step kinetics models to simulate diesel cold starting. However, there has not been any work that combines the optical diagnostics and multi-dimensional modeling to study

diesel cold starting. Therefore, an experimental and numerical study was carried out to simulate the diesel cold starting condition inside two single-cylinder optically accessible engines.

RESEARCH APPROACH

AVL engine setup - An AVL single-cylinder research diesel engine (520, with four-valve head) was uniquely converted for optical access in our laboratory. Figure 1 shows the schematic of the engine modification. Optical access is provided through a quartz window in the extended piston and through a transparent section in the cylinder wall. The extended piston is sealed with two oil-impregnated piston rings, similar to those used for reciprocating compressors, and by a steel-backed Teflon ring. The optical piston has a few different bowl dimensions. The one used for high-speed movies has a bowl which is 66.5 mm in diameter and 16.5 mm deep. For fluorescence and spray dropsize measurements, a shallow piston bowl of 80mm-by- 3mm is used, in order to make room for the laser light to align with or access the spray axis. Optical access through the mirror and piston window is therefore limited by the bowl size, which is either 66.5 mm or 80mm in diameter. The AVL 520 engine is equipped with many cylinder heads and injector designs. For the test results reported here, we used a four-hole injector centrally mounted in a four-valve cylinder head. The injector hole size is 0.355 mm in diameter, with a 80-degree injection tilt angle from the injector axis (i.e., 10 degree downward from horizontal plane). No. 2 diesel fuel is used in the experiment, except for PLIF measurement, in which dodecane doped with TMPD and Naphthalene is used. The injection system consists of a Bosch pump and a Lucas solenoid control system to control the number and the timing of injection. The solenoid is mounted on the injector using an adapter, in order to

direct the high pressure fuel flow to the injector when the solenoid is open, or bleed the fuel back to the fuel reservoir when the solenoid is close.

An air conditioning unit, capable of both heating and cooling, provides charge air to the intake manifolds. In order to measure precisely the cold starting conditions, intake air, and absolute manifold pressures (MAP) were monitored carefully during the tests; cylinder and fuel injection pressures were measured at every crank angle. The intake-air mass flow rate and the blowby mass flow rates were also carefully characterized by mass flow meters. The design on the extended piston actually simplifies the blowby flow measurement. Instead of measuring the crevice flow rate indirectly through the crankcase as is usually done, we measured the blowby flow rate directly at the view port of the extended cylinder.

This engine is suitable for sophisticated optical diagnostics but is constrained to limited consecutive fuel injections or firing. For the tests reported here, the number of fuel injections is limited to be one or two. Therefore, it only simulates the first one or two cycles when the engine wall is still cold. The engine is motored by a 30HP Reliance (type T) DC Dynamometer. During tests, the engine was motored to a fixed speed of 500 rpm before fuel injection commenced. The opening pressure of fuel injection is around 20 MPa. The amount of fuel injected was carefully calibrated for each injection by cycle-averaged over many injection under each conditions. The amount of the fuel injected was varied from 27 mg to 210 mg; the higher limit represents overfueling operations during starting. Due to the fuel-charging process of the solenoid adapter and the injector, the amount of the first injection is always smaller than the second one. By timing the solenoid opening in advance and away from the fuel pump pressure peak minimize but can not completely eliminate this effect. Being the first one or two injections, the injection

timing was found to vary slightly from the preset time for each test; therefore, the injection timing was determined from the fuel injection pressure.

LABECO engine setup - In addition, another TACOM/LABECO single-cylinder research diesel engine is retrofitted with mirror-coupled endoscope (AVL 510) access. It is located inside a micro-processor controlled cold room; therefore it can be operated under a wide range of practical engine conditions and is ideal for cycle-to-cycle variation study. Before starting the engine, it was soaked at the fixed ambient temperature condition for eight hours. The set up of the LABECO engine and cold room can be found in the Henein and Lee (1986). In order to provide for endoscope access in the cylinder head, the original injector was replaced with a Stanadyne single-hole pencil-type injector (Tolan and Hess, 1983), which has a hole diameter of 0.711mm and an opening pressure of 20 MPa. The geometric arrangement of the fuel injector and the endoscope on the engine is shown in Fig. 2. The amount of fuel injection was fixed at 12 mg in the experiments in order to prevent damage to the endoscope probe during continuous firing. Blowby measurements was also conducted for the LABECO engine, by measuring the air flow rate out of its crank case to the ambient. In addition to high speed movies data, luminosity from combustion flames was also measured using a photodiode, which was directly coupled to the endoscope and calibrated using an AVL calibration flash bulb. The specifications of the two engines are summarized in Table 1.

Table 1. Engine Specifications

OAE	Bore (mm)	Stroke (mm)	Comp. Ratio	Swirl Number	IVO (BTDC)	IVC (ABDC)	EVO (BBDC)	EVC (ATDC)
AVL 520	120	120	19.27	2.1	13°	26°	48°	6°
LABECO	114.3	114.3	16.5	0	20°	40°	50°	10°

Diagnostics - The experimental techniques used in this work are all optically based to resolve the highly temporal and spatial structures of the sprays. A 16 mm High-Speed Movie (Redlake Hycam) was used to directly visualize the global structures of the sprays and ignition process. A 1 kW studio lamp provided lighting to the spray through the optical windows for the AVL engine, but for the LABECO engine, lighting of the spray was provided through the endoscope using flash bulbs. From the high speed movies, the penetration of the fuel spray, the formation of luminous ignition spots, and propagation of the combustion are observed carefully and compared with multi-dimensional predictions.

To visualize the vaporizing diesel sprays, laser-induced exciplex fluorescence (LIEF) is used. The planar exciplex technique is described in Sun et al. (1993); it is based on the system developed by Melton (1988) and his coworkers to spectrally separate the liquid-phase fluorescence from the vapor-phase. Since oxygen quenches the monomer (vapor phase) fluorescence severely, the experiment is limited to a nitrogen environment and thus to non-reacting conditions. The laser light is expanded into a thin sheet using a cylindrical lens and is

aligned with the spray axis through a transparent section in the extended cylinder. For this technique, we used the third harmonic (355 nm) from the Nd-YAG laser (Spectra-Physics DCR-10) to obtain stronger quantum efficiency. As a result, the fluorescence image is strong enough for a 35-mm still camera or a cooled CCD camera (Photometrics CCD200) to record the instantaneous spray images. Therefore, spatial resolution is better than that obtained using an MCP-intensified camera. An Aerometrics two-component phase Doppler particle analyzer (PDPA) system was also employed to perform the simultaneous measurements of the droplet size and velocity. The PDPA measurements are used to validate the spray prediction. Due to limitation of this paper, the PDPA results will be described in a subsequent paper.

Spray and combustion Analysis - A modified version of KIVA-II (Amsden et al., 1989) developed by Los Alamos National Laboratory is used to simulate the spray and combustion processes. The mechanisms of the most interest here are the spray breakup, low temperature ignition kinetics, and blowby models. For comparison, the following three spray models were evaluated: the Taylor Analogy Breakup (TAB, O'Rourke, et al., 1987) without initial disturbance values (amp0), spray with prescribed initial dropsize and spray angle (i.e., without breakup submodel), and wave breakup model (Liu et al., 1993). To simplify comparison with other work, the spray injection velocity is taken from the correlation of Hiroyasu and Arai (1990). In addition to spray penetration calculated by KIVA, empirical correlations of spray structure by Dent (1971) and Hiroyasu and Arai (1990) were also compared with experiment. The multi-dimensional simulation results reported in this paper, however, are limited to the AVL engine, with a grid size of 20x20x20 for a quadrant of combustion chamber.

The ignition model is based on a modified Shell model to describe the pre-flame reactions, when the local grid temperature is below 100^0oK; however, when the temperature exceeds 1000 °K, a one-step Arrhenius kinetics model is applied to describe the high temperature reaction. The modification is described in Kong and Reitz (1993), and is also used in the current study. The combined models have been shown to properly account for the energy release during the autoignition event and the subsequent combustion process for a warm Cummins NH engine.

RESULTS AND DISCUSSION

The OAE combustion experiments showed that they can duplicate the combustion instability observed in many diesel engines during starting at low ambient temperature. Under appropriate engine conditions, the cold starting problem can be studied at near room temperature conditions, which greatly simplify the optical diagnostics. Table 2 and 3 summarize the test conditions for the two OAE's. They show that temperature is by far the most influential factor affecting ignition delay and heat release profile (Colella et al., 1987). It also demonstrates the behavior of a tight "critical temperature window" for starting, above which stable combustion can be initiated and below which combustion fails to take place. The combustion mode of the AVL engine in Table 2 is based on the cylinder pressure rise. However, even for cases where cylinder pressure traces show no significant heat release, high-speed movies sometimes still reveal a flash or spot ignitions.

AVL engine results - The critical temperature window for the AVL engine test is very narrow, ca. only about one or two degrees Kelvin. For the first three test groups (test number 1-25), the critical temperature window in the range of 288-289°K. However, a careful examination

shows that this window also depends sensitively on the injection timing and the amount of fuel injection. For example, Fig. 3(a) shows that delaying the fueling injection timing changes the combustion mode from misfiring in test No. 4 to successful firing in test No. 5. This is primarily due to the higher compressed air temperature for the later fuel injection case at the time of ignition. But at half the amount of fuel injected, similar change in the injection timing results into a reversed trend in test No. 15 and 16, as shown in Fig. 3(b). Fig. 3(b) also shows the cylinder pressure trace for a successfully fired test No. 17, whose intake temperature is only one degree Kelvin higher. This demonstrate a competition between the chemical (reaction rate) and the physical (fuel vaporization and mixing with air) processes.

From the limited two-injection tests conducted in test No. 22-32, the unstable combustion can be characterized by a misfiring following a successfully fired cycle or vice versa within the critical temperature window. Figs. 4 (a) and (b) show the cylinder pressure traces of test No. 22 and 23, which have two consecutive injection cycles under the critical temperature conditions. The first cycle of No. 22 is misfired although a flash was observed in the high-speed movies. The change in cylinder pressure between the first and second injection strongly suggests the effect of residual gas, which may affect both the temperatures and gas concentrations of the charge air for the second cycle. By fixing the inlet temperature, and varying the amount of fuel injections in test number 26-32, the window can be shown to occur at 293°K. Figure 5(a)-(c) show the cylinder traces of test No. 28, 31, and 32. The combustion mode change between 28 and 31 is primarily due to the compressed air temperature effect, but the first misfire cycle of test No. 32 is probably due to insufficient mixing with too small quantity of fuel-injected.

Table 2 Summary of AVL engine test conditions and their combustion modes

TEST NUMBER	INTAKE AIR TEMP. (^{o}K)	COMBUST. MODE (cylinder pressure)		MASS OF FUEL INJECTED (mg)		INJECTION TIMING (C.A. degree BTDC)	
		1st Cycle	2nd Cycle	1st Cycle	2nd Cycle	1st Cycle	2nd Cycle
1	286	Misfire	-	125	-	7	-
2	287	Misfire	-	125	-	10	-
3	287	Misfire	-	125	-	7	-
4	288	Misfire	-	125	-	9	-
5	288	Fire	-	125	-	5	-
6	289	Misfire	-	116	-	19	-
7	289	Misfire	-	119	-	10	-
8	290	Fire	-	125	-	8	-
9	291	Fire	-	125	-	10	-
10	291	Fire	-	125	-	8	-
11	292	Fire	-	125	-	7	-
12	293	Fire	-	125	-	8	-
13	296	Fire	-	125	-	7	-
14	299	Fire	-	125	-	6	-
15	288	Misfire	-	66	-	12	-
16	288	Fire	-	60	-	18	-
17	289	Fire	-	60	-	16	-
18	290	Fire	-	40	-	15	-
19	290	Fire	-	66	-	12	-
20	291	Fire	-	66	-	13	-
21	294	Fire	-	66	-	13	-
22	289	Misfire	Fire	50	55	25	25
23	290	Fire	Fire	50	55	25	25
24	291	Fire	Fire	50	55	25	25
25	292	Fire	Fire	50	55	25	25
26	293	Misfire	Misfire	190	210	25	25
27	293	Misfire	Misfire	164	180	25	25
28	293	Fire	Misfire	154	170	29	21
29	293	Fire	Fire	145	160	25	27
30	293	Fire	Fire	117	130	25	25
31	293	Fire	Fire	36	40	27	27
32	293	Misfire	Fire	27	30	24	24

These results demonstrated the sensitive nature of borderline firing during diesel engine cold starting. Therefore, OAE is a good tool for studying the diesel cold starting problem. The experimental data generated will be a strict test and challenge for low temperature pre-ignition kinetics submodels and multidimensional model which simulate regular diesel combustion.

One reason that the critical temperature window is relatively high for the AVL engine is because of its high blowby rate, since its compression rings are operated oil-free. Therefore, blowby measurement is critical for this study. Another reason is due to the fact that injection pump at low cranking speed can not generate high injection pressure. Therefore, the droplet diameter is expected to be large; the empirical correlation shows that the dropsize is about 21 microns. In addition, overfueling may reduce the compressed air temperature and therefore contribute to the higher range of the critical temperature window. However, high critical temperature is actually desirable in our experiment. It simplifies the experimental setup tremendously by simulating cold starting phenomena outside the cold room; therefore, we were able to perform optical diagnostics and probe the combustion chamber with relative ease.

Fig. 6 show the luminous and pressure rise time delays (with respect to the start of fuel injection) for the two engines, as a function of the ambient air temperature, for test No. 5-14. The luminous time delay is determined at the point when luminous spots are observed in the high-speed movies. The pressure rise delay is determined at the point when the cylinder pressure deviates from a smooth decaying curve similar to that in the motoring case. Even for cases with misfire, high-speed movies sometimes still reveal luminous spots. Although there is uncertainty involved in determining these time delays, the luminous delay is consistently longer than the pressure rise delay. This observation shows the presence of preflame exothermic reactions. The

difference between these luminous and pressure rise delays is approximately 2 ms. The reason why pre-flame reaction is observed for AVL engine even at 299 °K may be due to its large blowby.

Fig. 7 shows a sequence of high-speed movies of a successfully fired cycle of test No. 9, at 291°K ambient temperature. The framing rate for the camera is approximately 5,000 frame per second (fps), but only one out of every four frames of the film clip is shown for brevity. The luminous ignition occurs after fuel injection is completed, usually at more than one location. The combustion cycle is not as intense as a warm engine cycle, and is characterized by spotted combustion mode, especially in early and late in the combustion cycle as shown in the movies.

LABECO engine results - Fig. 8 shows the high-speed movies of the first two cycles after fuel injection started for LABECO engine operated at 283 °K. Although both cycles were successfully fired, the second cycle showed incomplete combustion. This is evident by its much lower flame luminosity and peak cylinder pressure. The cylinder pressure and luminosity traces of ten consecutive cycles for test No. 1,2 and 4 are shown in Figs. 9 and 10. At high temperature condition, the combustion is stable as demonstrated by the more repeatable and tightly packed cylinder pressure and luminosity traces in Figs. 9(a) and 10(a). The data acquisition was triggered a few cycles after fuel injection, therefore the first cycle shown is not the first fuel injection.

Table 3 Summary of LABECO engine test conditions and their combustion modes

TEST NUMBER	INTAKE AIR TEMP. (^{o}K)	COMBUSTION MODE	MASS OF FUEL INJECTED (mg)	INJ. TIMING (C.A. degree BTDC)
1	298	Stable	12	16
2	293	Stable	12	16
3	283	Less stable	12	16
4	278	Borderline	12	16
5	268	Misfire	12	16

At the ambient temperature of 293 ^{o}K, the flame luminosity peaks are consistently lower than those of the 298^{o}K case, denoting less intense combustion. The luminous ignition delays are also longer and have a wider scatter. A misfire based on cylinder pressure trace seem to occur at cycle No. 3. At the ambient temperature of 278 ^{o}K, more misfire seem to occur. The luminosity levels are more sporadic; some of them even have higher luminosity than those of the higher temperature cases. Although the amount of heat release is insignificant from the cylinder peak pressure for these misfire or incompletely combustion cases, exothermic reactions obviously took place, as is evidenced by the tail end of the cylinder pressure. The presence of luminosity in each cycle shows that autoignition takes place in every cycle; therefore, its variation is caused by flame propagation processes. The highest peaks observed for the borderline conditions of 278 ^{o}K ambient temperature case are therefore, attributed to longer ignition delays at lower compressed air temperature and better prepared fuel-air mixture, which was also aided by the liquid fuel film vaporization left over from the previous cycle.

The fact that a misfire or incomplete combustion cycle follows a successfully fired cycle is intriguing but its reasons remain unclear. One possible explanation is that, due to the negative

temperature coefficient of ignition delay, especially for low Cetane number fuel higher, in the 650-750 ^{o}K range and the acceleration of the engine speed after one successfully firing, the ignition and combustion of the second cycle actually suffer because it has slightly higher compression temperature but less time to consume the radical and branching agents produced in the first stage of ignition reaction. Recent studies in flame reactors and research engine also showed that small concentrations of nitric oxide (NO) can alter the pre-ignition oxidation behavior of hydrocarbons, in particular, alkanes (e.g., Prabhu et al., 1995). Therefore, it also offers another possibility; i.e., the residual NO produced in the first firing cycle, instead of promoting reaction with HO_2 radical, serves as OH radical scavenger and causes major swing in the reactivity of second cycle. However, this effect depends strongly on the underlying fuel oxidation chemistry and the concentration of the residual NO, which remain to be determined.

Fig. 11 plots the measured luminous delays (with respect to the start of fuel injection) for the cases shown in Fig. 10 as a function of the ambient air temperature. The luminous time delay is determined at the point when luminous spots are observed in the high-speed movies. The pressure rise delay is less obvious and is therefore not shown. However, the luminous delay is consistently longer than the pressure rise delay determined by heat release calculations, suggesting the presence of the preflame exothermic reactions. However, the difference between these two delays trends to decrease with an increase in the ambient temperature.

Laser diagnostic and KIVA simulation results - The effects of air temperature and engine speeds on the intake and blowby flow rates are shown in Figs. 12 and 13 for the AVL engine. The instantaneous blowby measurement has a significant phase delay with respect to the cylinder pressure; therefore, only the averaged blowby measurements are shown. The blowby

flow rate of the AVL engine is about 6 to 8 percent of input charge air for the temperature ranges tested, showing an increasing trend with decreasing intake air temperature. The blowby flow rate is used to benchmark a blowby submodel in KIVA (Reitz and Kuo, 1989), whose results are also shown in the figures. The blowby model is calibrated at the low temperature end (287°K), and shows a similar decreasing trend as the intake air flow rate. However, the slope is not as steep as the measured blowby flow rate. This may be due to the model assumption that air within the crevice is in thermal equilibrium with the cylinder wall; however, changing the cylinder wall temperature from 300 to 350°K does not show big effect. Therefore, other reasons which require further study, may have contributed to the temperature sensitivity of blowby. The measured blowby rate for the LABECO engine is much smaller, around 3-4 percent at 500 rpm (Henein and Lee, 1986). However, both engines show that both the intake and blowby flow rate increase with decrease in engine speed and decrease in ambient temperature. This is consistent with previous studies (Henein and Lee, 1986; Gonzalez et al., 1991). Fig. 14 shows predicted and measured cylinder pressures under motoring conditions. Using the calibrated blowby model, KIVA can predict the measured peak cylinder pressure trace at the calibration point fairly well, but lacks the sensitivity with respect to change in air temperature. It also overpredicts the cylinder pressure in the expansion stroke.

Fig. 15 shows the normalized filtered LIEF visualization of vaporizing spray at 0.9 and 1.6 ms after fuel injection. The liquid phase signal is significantly stronger than the vapor phase, especially at 0.9 ms, where less fuel vapor was present. The weaker vapor phase fluorescence has a much smaller dynamic range; therefore the cylinder head background becomes visible when the image intensity is normalized. When compared with the liquid spray data from high-speed movie, there is no significant difference in the spray penetration. However, the vapor-

phase spray angle is significantly larger than the liquid-phase one. In addition, the effect of swirl convection transport is more obvious for the vapor phase. The liquid-phase fluorescence has been known to shift up toward the vapor-phase at higher temperature. This temperature sensitivity of the liquid phase will make quantitative interpretations of LIEF results difficult in a highly inhomogeneous temperature field such as in a diesel spray. Another problem is that cross-talk between the fluorescence of the two phases will make phase discrimination difficult. This difficulty has been a concern, especially for temperatures above 600°K. Therefore, the strength of this technique is primarily qualitative and is used to validate the liquid and vapor front penetration.

Fig. 16 shows a typical PDPA measurements of diesel spray at 30 mm from the injector for test conditions 22. The data is cycle-averaged over the two injections. Data date is low due to difficult optical access, the high droplet density of the diesel spray, and the stringent test criteria of a 2-D PDPA. High-velocity spray front is not well captured; only the long and slow spray tail is better described. The maximum spray velocity measured is around 40 m/s, equivalent to the averaged spray penetration speed at this speed. When longer injection duration was used, two separate injections from the injector were sometimes observed in the high-speed movies. The PDPA measurements also capture the multiple injections and injector dynamics. The measured dropsize is fairly large, with a SMD of about 40 microns. More measurements are required to validate the multidimensional prediction of diesel sprays during starting.

Fig. 17 shows the comparison of the predicted spray penetrations of test No. 2, using three commonly used spray breakup models. The spray trajectories with its represented dropsizes are visualized from two perspectives (top and side views), at 1, 2, 3 and 4 degree after

fuel injection. The smaller drops are convected more in the swirling flow direction but not the bigger ones. The dropsize after impingement also increases due to coalescence. However, after impingement, most of the spray droplets, instead rebounding, spread along the piston bowl wall. The comparison of the measured and predicted penetration is shown in Fig. 18. It shows that all three spray models perform reasonably well, but all three models tend to overpredict spray penetrations initially. Since proper injection velocity is required for any breakup model to successfully predict the spray penetration, the overprediction is therefore due to the high initial injection velocity specified using empirical correlation.

The reason why one model is predicting better than another can be understood by comparing Fig. 17 and 18. Similar to what other researchers have found at higher pressure case, the baseline TAB model (i.e., zero amp0) overpredicts atomization of the low pressure diesel, thus overpredicts the swirl effects and underpredicts the spray penetration. The spray model with assumed initial dropsize and spray angle based on empirical correlation shows best agreement with the penetration measurements; the predicted dropsize also seems to agree better with the measured one. But the spray structure near the injector may not be correctly represented. The wave breakup model predicts poor atomization and generates only very small satellite droplets, which follow the swirling flow. Therefore, it overpredicts the penetration even later in the and may underpredicts fuel vaporization for the low pressure diesel spray in this experiment. Fig. 18 also shows that the empirical correlations do not predict well the penetration of the low pressure diesel spray typically observed during cold start. The lack of good prediction (i.e., overpenetration) of empirical correlations is also observed by Friz and Abata (1987). Therefore, the applicability of empirical correlations developed for the high engine-speed, high pressure spray to diesel starting conditions is limited.

Fig. 19(a) shows the cylinder pressures predicted by KIVA using the wave breakup model under 287 °K (test No. 2) and 299 °K (test No. 14) intake air conditions, with or without the blowby models. The measured cylinder pressure with fuel injection (first cycle) is also shown for comparison. Without the blowby model, KIVA predicts a successful autoignition and combustion for both temperature conditions. With the blowby model, KIVA predicts the peak pressure fairly well for the 287 °K case but underpredicts the peak pressure for the 299 °K case. This is due to the overprediction of blowby flow rate as discussed earlier. Although a small amount of heat release is observed, KIVA underpredicts the observed heat release rate for the 287 °K case and fails to predict the autoignition and deflagration for the 299 °K case. The effect of blowby model on the predicted mass-averaged temperature is shown in Fig. 19(b). The difference in peak compressed air temperature between a firing and a misfiring cycle is very small; this shows the sensitivity of the pre-ignition chemistry submodel to the blowby submodel .

Fig. 20(a) shows the effect of the amount of fuel injected on the measured cylinder pressures for AVL engine test No. 7 and 17, and their predictions using KIVA. KIVA correctly predicts a misfire in test No. 17 and the successfully fired case of test No. 17. The peak pressures for both cases which have the same intake air temperature of 289 °K, however, were underpredicted. The measured peak pressure of test No. 17 is much higher, suggesting faster combustion rate or more fuel vaporized. The data for the misfired case clearly points to the latter, which may be due to the underprediction of atomization by the wave breakup model. The predicted mass-averaged air temperatures are shown in Fig. 20(b) to have shows little difference, further confirming the conclusion that the discrepancy between the prediction and the measurement is rather on the breakup model than on the chemistry model.

Figs. 21(a) and (b) shows the effect of fuel injection timing on the predicted cylinder pressures, and the mass-averaged air temperatures for an hypothesized AVL engine test case. The intake air temperature is taken to be 289 ^{o}K and the amount of fuel injection, 0.08g. The prediction based on wave breakup model. The results show that although advancing the injection timing produces a lower peak temperature, but the fuel-air mixture is better prepared for auto-ignition. This again shows the sensitivity of the pre-ignition chemistry submodel. Therefore, more validation work is required to clarify the interaction of pre-ignition chemistry with diesel physical processes (e.g., spray, blowby, and heat transfer models) and engine dynamics (friction and engine speed).

CONCLUSIONS

In part I, an application of two optical accessible engines to study the diesel cold starting is described. The current capability of using multi-dimensional calculation using multi-step kinetics model to simulate diesel cold starting is also evaluated. The conclusions are summarized as follows:

- OAE is a good tool for studying the diesel cold starting problem. It can duplicate the combustion instability within a "critical temperature window" observed in many diesel engines during cold starting. In this paper the performance of two OAE's are demonstrated: one is ideal for sophisticated optical diagnostics; the other is suitable for characterizing cycle-to-cycle variation.

- The combustion stability during cold starting is very sensitive to the engine operation conditions, and involve competing physical and chemical processes. The experimental data

show that ambient temperature is by far the most dominant parameters; however, amount of fuel injection, injection timing, combined with blow-by flow and residual gas effects can modify the combustion mode. Therefore, OAE cold starting experiments provide challenging data for validating low temperature pre-ignition kinetics submodels, as well as multidimensional model which simulate normal diesel combustion.

- Under appropriate engine conditions, the cold starting problem can be studied at near room temperature conditions, which greatly simplify the optical diagnostics. In our experiments, the combustion instability is observed between 288-293°K at 500 rpm for AVL engine operated under one or two fuel injection conditions.

- Pre-flame exothermic reactions were observed by the fact that luminous delay is consistently longer than the pressure rise delay.

- Current multi-dimensional code like KIVA with many of its key submodels in place can do a satisfactory job of simulation the general trends observed in the experiment.

- The blowby flow rate is critical for cold starting study. Both experiments and simulations show a dramatic increase with decrease in engine speed. They also show a slight increasing trend with decreasing intake air temperature. Using a calibrated blowby model, KIVA can predict the measured peak cylinder pressure fairly well. However, current blowby underestimated the temperature effect.

- LIEF visualization of vaporizing spray is qualitatively useful in diesel cold starting study in showing the location of the liquid and vapor phases of the fuel.

- PDPA measurement can capture the diesel spray dynamics and multi-stage injection at low cranking speed, but more measurements are required to validate the multidimensional prediction of diesel sprays during starting.

- Baseline TAB model overpredicts spray atomization of the low pressure diesel spray, thus overpredicts the swirl effects and underpredicts the spray penetration. The spray model with assumed initial dropsize and spray angle based on empirical correlation shows best agreement with the penetration measurements. The wave breakup model predicts poor atomization and may underpredict fuel vaporization for the low pressure diesel spray in this experiment. Proper injection velocity is required for any breakup model to successfully predict the spray penetration.

- Empirical correlations developed for the high engine-speed, high pressure spray do not predict well the penetration of the low pressure diesel spray typically observed during cold start. Therefore, their applicability to diesel starting conditions is limited.

- The pre-ignition chemistry is very sensitive to compressed air temperature, blowby flow rate, wall temperature, and heat transfer rates. Therefore, more validation work is required to clarify the interaction of pre-ignition chemistry with other diesel engine physical processes and engine dynamics (friction and engine speed).

PART II: Determination of Ignition Delay in Diesel Engines from Constant Volume Vessels Data

ABSTRACT

Many investigations on the autoignition of diesel fuels have been conducted in constant volume vessels under gas pressures and temperatures which simulate the conditions in actual engines. The data obtained for the ignition delay (ID) under these conditions have been found not to agree with the data obtained in engines under actual running conditions. This paper presents a method to compute the ID in engines from data obtained in constant volume vessels. The method accounts for the effect of variations in charge pressure and temperature on the formation of the chain carriers from the combustible mixture during the ID period. A comparison is made between the computed ID and data obtained in a research direct injection diesel engine under different ambient temperatures ranging from 20 C to - 10 C.

INTRODUCTION

The ID in diesel combustion is one of the parameters which affect engine power, fuel economy, exhaust emissions of hydrocarbons, nitrogen oxides and soot particulates (Heywood 1988). Further more, the rate of pressure raise at the end of the ID, and the peak cylinder gas pressure are directly related to the mass of the premixed charge which depends, to a great extent, on the length of the ID period. High rates of pressure rise and peak pressures may results in excessive engine noise and vibration, in addition to increased mechanical and thermal stresses.

ID data are needed for the diesel engine cycle-simulation and for the design of combustion chambers for high power-density engines that can run on regular as well as alternate fuels. Many ID data are the result of investigations conducted in constant volume vessels under steady state conditions of air pressure, temperature and charge motion (Arai *et al* 1984, Fujimoto *et al* 1979, Hoskin *et al* 1992, Parker *et al* 1985, Ryan III and Callahan 1988). These investigations are desirable because they deal with a limited number of controlled variables, consume less time and are less expensive to run than experiments conducted on actual engines (Hamanoto *et al* 1993, Hardenberg and Hass 1979, Henein and Bolt 1969, Xia and Flanagan 1987). However, there has always been discrepancies between the data obtained in engines and under steady state conditions. The goal of part II is to introduce a method to compute the ID in engines from data obtained in constant volume vessels. The computed results are compared with experimental data obtained on an actual research engine at ambient temperatures ranging from 20 C to - 10 C.

RESEARCH APPROACH

Comparison between the conditions in constant volume vessels and engines - The main difference between the conditions in constant volume vessels and engines is the continuous variation in the volume of the charge caused by piston motion, and the corresponding changes in pressure and temperature. As an example, Figure 1 shows two pressure traces: A and B, which are obtained in the engine used in the present investigation, at ambient temperatures of 20 C and - 10 C respectively. In case A, the ID ended during the compression stroke while energy is added to the charge by the piston motion. This causes an increase in pressure and temperature during ID period. This is not the condition in case B, where the piston motion during the

expansion stroke resulted in a drop in the charge pressure and temperature near the end of ID. In constant volume vessels, the charge remains at a steady pressure and temperature during ID period (Edwards *et al*, 1992).

Correlation of ID in constant volume vessels and engines - In order to arrive at a correlation between the ignition delay in constant volume vessels and engines, reference is made to the previous work done by Livengood and Wu (1955) in predicting knock in S.I. engines from data obtained in a rapid compression machine. They reported that the pressure and temperature at the end of compression in the machine remained constant during the ID, while they changed in the engine. The basic concept in their work is that, in the two cases, the concentration of the chain carriers increases during the ID period and autoignition occurs when a critical concentration $[C_c]$ is reached. The ratio of production of the chain carriers to the critical concentration was related to the ratio of time t, elapsed after the start of the reaction and the total ignition delay period τ.

$$d([C]/[C_c])/dt = \phi(t/\tau) \qquad (1)$$

If the reaction rate is assumed not to change with time, because of the constant pressure and temperature, they concluded that equation (1) becomes

$$[C]/[C_c] = \int_{t=0}^{t=t_{ig}} \frac{1}{\tau} dt = 1 \qquad (2)$$

The conditions of the charge leading to autoignition in diesel combustion are quite different from those leading to knock in gasoline engines. The charge in diesel engines is extremely heterogeneous, particularly during ID, compared to the homogeneous charge in the knock zone

of the gasoline engines. To account for this, the model in the present investigation considers the following:

1. A small volume of the charge autoignites first and starts the combustion process.
2. The average equivalence ratio in this volume is around the stoichiometric mixture.
3. This volume is composed of specially distinct small heterogeneous elements which successively form a combustible mixture and start forming chain carriers.
4. All the elements contribute in a cumulative manner to the critical concentration of the chain carriers which is required to produce autoignition at the end of ID.

To account for the variation of pressure and temperature for the different elements in the engine, the total ignition delay time is divided into several small time intervals, during each of which the pressure and temperature are assumed to remain constant. And the rate of increase of the concentration of the chain carriers [C] is given by

$$d([C]/dt = \beta \tag{3}$$

Where β is a constant. Accordingly, the concentration of the chain carriers produced from each element can be calculated at the end of each time increment, up to the end of ID period. The first element has the longest time, while the last element has the shortest time. To illustrate this analysis, consider a case in which the total ignition delay is divided in three equal intervals time t_1, t_2, t_3 and a fraction of an interval t_{ig} as illustrated in Fig. 2. From equation (3), the concentration of chain carriers produced from any element m after increment of time n can be given by

$$[C_c]_m = \beta_n t_m \tag{4}$$

The total concentration of chain carriers $[C_{ig}]_m$ from all the elements at the end of the ID period is,

$$[C_{ig}]_1 + [C_{ig}]_2 + [C_{ig}]_3 + [C_{ig}]_4 = \beta_1 t_1 + \beta_2 t_2 + \beta_3 t_3 + \beta_4 \Delta t_{ig} \qquad (5)$$

Since $t_1 = t_2 = t_3 = t$ and $0 < t_{ig} \leq t$, a general form of the equation (5) becomes

$$\sum_{i=1}^{n} [C_{ig}]_i = \beta_1 t + 2\beta_2 t + 3\beta_3 t + \ldots\ldots + (n-1)\beta_{n-1} t + n\beta_n \Delta t_{ig} \qquad (6)$$

β_i can be substituted for by considering the relationship between the critical concentration $[C_c]$ and the ignition delay τ_i measured in the vessel at the average pressure and temperature.

$$\beta = [C_c] / \tau_i \qquad (7)$$

And since the ratio of chain carriers concentration under engine conditions and vessel conditions should be equal to 1 when autoignition occurs, equation (6) and (7) give:

$$\sum_{i=1}^{n} [C_{ig}]_i / [C_c] = (t_1 / \tau_1) + 2(t_2 / \tau_2) + \ldots\ldots + (n-1)(t_{n-1} / \tau_{n-1}) + n(\Delta t_{ig} / \tau_{ig}) = 1 \qquad (8)$$

Equation (8) can be put in the following form.

$$\varphi_n(t) = (t_1 / \tau_1) + 2(t_2 / \tau_2) + \ldots\ldots + (n-1)(t_{n-1} / \tau_{n-1}) + n(\Delta t_{ig} / \tau_{ig}) = 1 \qquad (9)$$

where t / τ represents a dimensionless increment of time. The general form of equation (9) is,

$$\sum_{i=1}^{n-1} (i \times t / \tau_i) + n(\Delta t_{ig} / \tau_n) = 1 \qquad (10)$$

Where n is the number of time increments, t is the time increment, τ is the ignition delay calculated from vessel data for the same fuel, at the mean pressure and temperature during each time increment.

In diesel combustion the main factors which affect the autoignition reactions are gas temperature and pressure, which change in the engine during the ignition delay period. It is assumed that the fuel is the same in both the vessel and the engine. Another difference between the two cases is the gas motion which is more in engines than in vessels. Swirl and tumble motions produced in the engine during the intake stroke continue in the compression stroke and contribute to turbulence in the combustion chamber, as the fuel is injected near the end of the compression stroke. It is well established that the turbulence affects the mixing of fuel spray and the combustion of the bulk of charge. But since diesel ignition starts in a small area and spreads to the bulk of the spray, it is expected that the gas motion will have a small effect on ID. This is based on the fact that in automotive type diesel engines the so called physical delay does not play a major part in the total delay period.

Experimental set-up - The engine used in this study is a TACOM research single cylinder DI engine located in a cold room. The engine has 114.3 mm (4.5 in) cylinder bore, 114.3 mm (4.5 in) stroke and a compression ratio of 16:1. It has a Bosch injection nozzle with 4 holes each has 0.2977 mm (0.0118 in) in diameter. The opening pressure of 20685 is kPa (3000 psi). The cylinder pressure is measured by a flush mounted quartz pressure transducer. The needle lift and fuel line pressure are measured by a Bentley Nevada 3000 sensor and an AVL strain gage type pressure tranceducer respectively. The mass of intake air to the engine is

measured by a Meriam laminar flow meter. The engine is connected to a General Electric D.C. Motor/Generator cradle type dynamometer. Engine speed and TDC signals are obtained by a shaft encoder. Experiments were conducted at various ambient temperatures ranging from 20 C to -30 C. The data was recorded when the engine reached steady state at 500 rpm. Diesel fuel was injected at a rate of 21 mg per cycle.

RESULTS AND DISCUSSIONS

Test results - Ignition delay period defined here is the time from the start of fuel injection to the point where a change in the pressure trace occurs due to autoignition and combustion. The temperature is calculated by the equation of state. The effect of the ambient temperature on the ignition delay is shown in Fig. 3.

Calculation of $\psi_n(t)$ Function - The ignition delay in constant volume vessel is calculated from a correlation developed by Igura *et al.* (1979) for diesel fuel of the same cetane number as the fuel used in the present study. The data is shown in Fig.4 as iso-delay lines over a map covering the range of air pressures and temperatures of interest in this investigation. The temperature and pressure path followed by the charge in the experimental engine, from the start of fuel injection to autoignition, is superimposed on the iso-delay lines. The experimental data shown is for ambient temperatures varying from 20 C to -10 C. It is observed that the variation in charge temperature and pressure increase with the increase in ID at the lower ambient temperatures.

According to equation (9), autoignition occurs if the sum of the contributions of the different elements produces the critical concentration of the chain carriers. Figure 5 shows the

result of the computed function $_n$, for the different ambient temperatures, as a function of the elapsed time from the start of injection. The time at which $_n$ reaches unity is considered the end of the computed ID. A sample of the computations, at - 10 C is given in the Appendix. Figure 6 shows a good agreement between the ID computed from the constant volume vessel and that measured in the engine. At ambient temperature -10 C, the final value of $_n$ is 0.995. The other final values are 1.008, 0.995 and 1.005 for ambient temperatures 0 C, 10 C and 20 C respectively. The error is between + 0.8 % and - 0.5 %.

CONCLUSIONS

1. A method has been developed to calculate the ignition delay period in diesel engines from data obtained on the same fuel in a constant volume vessel. The method accounts for the effect of the temporal variations in gas pressure and temperature on the autoignition reactions during the ignition delay period.

2. The ignition delay period (t_{ig}) in diesel engines is related to the ignition delay period in constant volume vessels by the following equation:

$$\sum_{i=1}^{n-1} (i \times t / \tau_i) + n(\Delta t_{ig} / \tau_n) = 1$$

$$0 \le \Delta t_{ig} \le t$$

   Where Δt_{ig} is a residual time, which is shorten than t.

3. The computed ignition delay period showed a fairly good agreement with that measured in a direct injection diesel engine at different ambient temperature, ranging between -10 C and 20 C. The error is within ± 1.0 %.

A sample of twenty four dimensionless time increments for the run at an ambient temperature of - 10 C is as follows.

$$\psi_{24} = 0.099 \times \{(1 / 48.349) + (2 / 46.111) + (3 / 44.008) + (4 / 42.026) + (5 / 40.155)$$
$$+(6 / 38.383) + (7 / 36.702) + (8 / 35.102) + (9 / 33.578) + (10 / 32.123) + (11 / 30.731)$$
$$+ (12 / 29.784) + (13 / 29.434) + (14 / 29.061) + (15 / 28.664) + (16 / 28.242)$$
$$+ (17 / 27.794) + (18 / 27.322) + (19 / 26.553) + (20 / 25.242) + (21 / 23.979)$$
$$+ (22 / 22.762) + (23 / 21.590)\} + 24 \times (2.28 - 2.277) / 20.49$$
$$= 0.995$$

More detailed calcalation of $\varphi_n(t)$ is described in the appendix.

LIST OF PUBLICATIONS

Lai, M.-C., Henein, N. A., Xie, X., Chue, T.-H., Itoh, Y. and Bryzik, W., (1995) "Diesel Spray Behavior under Cold-Starting Condition," ILASS-95, May 21-24, Troy, Michigan.

Lai, M.-C., Henein, N. A., Xie, X., Chue, T.-H., Itoh, Y. and Bryzik, W., (1995) "Diesel Cold-Starting Study using Optically Accessible Engines," Int'l SAE Fuels and Lubricants Meeting, Toronto, Oct. 16-19, 1995, SAE paper 952366.

Lai, M.-C., Li, L. and Xie, X., (1997) "Angular Dependence of OH Degenerate Four-Wave Mixing Signals in a Flame," *Optics and Lasers in engineering*, Vol. 28(3), pp. 229-235.

Itoh, Y., Henein, N. A., and Bryzik, W. (1997) "Determination of Ignition Delay in Diesel Engines from Constant Volume Vessels Data," ASME ICE Division Spring Technical Meeting, Fort Collins, CO, April 27-29, 1997.

LIST OF PARTICIPATING SCIENTIFIC PERSONNEL EARNING ADVANCED DEGREES

1. Daniel T.-H. Chue, Ph.D., 1994, currently at General Dynamics Land Systems, Warren, Michigan
2. Yasuhiko Itoh, Ph.D., 1997, currently at Wayne State University

ACKNOWLEDGMENTS

The authors acknowledge contributions from the following graduate students and research staff: Daniel Chue, Yasuhiko Itoh, Xingbin Xie, and Huimin Sun. We also thank Dr. Walter Bryzik of U.S. TARDEC for his technical support, and Prof. R. D. Reitz for his kind assistance in providing submodels in the KIVA program.

REFERENCES

- Abraham, J., and Bracco, F. V. (1993) "Simple Modeling of Autoignition in Diesel Engines for 3-D Computations," SAE paper 932656.
- Amsden, A. A., O'Rourke, P. J., and Butler, T. D. (1989) "KIVA-ll: A Computer Program for Chemical Reactive Flows with Sprays," Los Alamos Report LA-11560-MS.
- Arai, M,. Higuchi, G., and Hiroyasu, H., 1984 " Ignition Delay of Diesel Fuel and Composite Fuels," Trans. Japan Soc. Mech. Engrs, Vol. 50, no. 453, pp. 1345 - 1352.
- Bardsley, M. E. A., Felton, P. G. and Bracco F. V. (1988) "2-D Visualization of Liquid and Vapor Fuel in an I, C. Engine," SAE paper 880521.
- Bryzik, W., and Henein, N. A. (1994) "Fundamental Cold Start Phenomena within Advanced Military Diesel Engines," in Proceedings of 19th Army Science Conference, June 20-23, 1994, Orlando, Florida.
- Colella, K. J., Balles, E. N., Ekchian, J. A., Cheng, W. K., and Heywood, J. B. (1987) "A Rapid Compression Machine Study of the Influence of Charge Temperature on Diesel Combustion," SAE paper 870587.
- Dale, J. D., Wilson, J. D., Santiago, J., Smy, P., and Clements, R. (1985) "Low Temperature Starting of Diesel Engines using Timed Spark Discharge," SAE paper 850049.
- DeCarolis, J. J., Meyer, W. E., and Espenschade, P. W., (1959) "Priming Aids for Cold Starting Diesel engine Engines," SAE Transaction, Vol. 67, pp. 351-364.
- Dent, J. C., (1971) "A Basis for the Comparison of Various Experimental Methods for Studying Spray Penetration," SAE Transaction Vol. 80, paper number 210571
- Edwards, C. F., Siebers, D. L., and Hoskin, D. H., (1992) "A Study of the Autoignition Process of a Diesel Spray via High Speed Visualization," SAE paper 920108.

- Fritz, S. G., and Abata, D. L., (1987) "A Photographic Study of Cold Start Characteristics of a Spark Assisted +-Diesel Engine Operating on Broad Cut Diesel Fuels," SAE paper 871674.
- Fujimoto, H,. Shimada, T., and Sato, G., 1979 " Study of Diesel Combustion in a Constant Volume vessel," Trans. Japan Soc. Mech. Engrs, Vol. 45, no. 392, pp. 599 - 609.
- Gonzalez, M. A., Borman, G. L., and Reitz, R. D., (1991) "A Study of Diesel Cold Starting using both Cycle Analysis and Multidimensional Calculations," SAE 910180.
- Hamamoto, Y., Tomita, E., Matusoka, Y., and Hirata, M., 1993 " Study on a Method for Measuring Ignitability of Diesel Fuel," The 11th Internal Combustion Engine Symposium, Japan No 79 pp.463-468.
- Hardenberg, H. O., and Hass, F. W., 1979 " An Empirical Formula for Computing the Pressure Rise Delay of a Fuel from Its Cetane Number and from the Relevant Parameters of Direct-Injection Diesel Engines," Soc. Auto. Engrs. Paper no. 790493.
- Henein, N. A., and Bolt, A., 1969 "Correlation of Air Charge Temperature and Ignition Delay for Several Fuels in a Diesel Engine" Soc. Auto. Engrs. Paper no. 690252.
- Henein, N. A. (1986) "Starting of Diesel Engines: Uncontrolled Fuel Injection Problems," SAE paper 860253.
- Henein, N. A., and Lee C.-S. (1986) "Autoignition and Combustion of Fuels in Diesel Engines under Low Ambient Temperature," SAE paper 861230.
- Henein, N. A., Zadeh, A. R., Yassine, M. K., and Bryzik, W. (1992) "Diesel Engine Cold Starting: Combustion Instability," SAE paper 920005.
- Henein, N. A. (1993) "Diesel Cold Starting: A Phenomenological Model," ASME ETCE Conference, Jan. 31- Feb. 3., 1993, Houston, TX.

- Heywood, J. B., 1988 Internal Combustion Engine Fundamentals : McGrow-Hill Book Company.
- Hiroyasu, H., and Arai, M. (1990) "Structure of Fuel Sprays in Diesel Engines," SAE paper 900475.
- Hoskin, D. H., Edwards, C. F. and Siebers, D. L. (1992) "Ignition Delay Performance versus Composition of Model Fuels," SAE paper 920109.
- Igura, S., Kadota,T., and Hiroyasu, H.. 1975 " Spontaneous Ignition Delay of Fuel Sprays in Pressure Gaseous Environment," Trans. Japan Soc. Mech. Engrs, Vol. 41, no. 345, pp. 1559 - 1566.
- Kawamura, H., and Yamamoto, S. (1983) "Improvement of Diesel Engine Startibility by Ceramic Glow Plug Start System," SAE paper 830580.
- Kobayashi, A., Suzuki, T., and Nakajime, M., (1980) "Combustion Analysis of the Vehicle Diesel Engine in Cold Starting Condition via High-Speed Photography," ASME paper 80-DG-7.
- Kong S.-C., Ayoub, N., and Reitz, R. D., (1992) "Modeling Combustion in Compression Ignition Homogeneous Charge Engines," SAE paper 920512.
- Kong S.-C., and Reitz, R. D., (1993) "Multidimensional Modeling of Diesel Ignition and Combustion Using a Multi-step Kinetics Model," J. of Engineering for Gas Turbines and Power, 115(4) pp.
- Lai, M.-C., Zhao, F.-Q., Amer, A. A., and Chue, C.-H. (1994a), "The Structure of Port Injector in Gasoline Engines," *Proceedings of International Symposium on Advanced Spray Combustion (ISASC)*, Hiroshima, Japan, July 6-8, 1994, pp. 79-89.

- Lai, M.-C., Zhao, F.-Q., Amer, A. A., and Chue, C.-H. (1994b), "An Experimental and Analytical Investigation of the Spray Structure from Automotive Port Injectors," *SAE Technical Paper*, No. 941873.
- Lai, M.-C., Henein, N. A., Xie, X., Chue, T.-H., Itoh, Y. and Bryzik, W., (1995) "Diesel Cold-Starting Study using Optically Accessible Engines," Int'l SAE Fuels and Lubricants Meeting, Toronto, Oct. 16-19, 1995, SAE paper 952366.
- Livengood, C. J., and Wu, C. P,. 1955 " Correlation of Autoignition Phenomenon in Internal Combustion Engines and Rapid Compression Machines," Proceeding of fifth International Symposium on Combustion, P.347, Reinhold.
- Liu, A. B., Mather, D., and Reitz, R. D., (1993) "Modeling the Effects of drop Drag and Breakup on Fuel Sprays," SAE 930072.
- Melton, L. A. (1983) "Spectrally Separated Fluorescence Emissions for Diesel Fuel Droplets and Vapor," Appl. Opt., 22, 2224.
- Murayama, T., Miyamoto, N., Chikahisa, T., and Ogawa, H. (1983) "Elimination of Combustion Difficulties in a Glow Plug-Assisted Diesel Engine Operated with Pure Ethanol and Water-Ethanol Mixtures," SAE paper 830373.
- O'Rouke, P. J., and Amsden, A. (1987) "The TAB Method for Numerical Calculation of Spray Droplet Breakup," SAE 872089.
- Parker, T. E., Forsha, D. M., Stewart, E. H., Hom, K, Sawyer, R. F., and Oppenheim, A. K., 1985 " Induction Period for Ignition of Fuel Sprays at High Temperatures and Pressures," Soc. Auto. Engrs. Paper no. 850087.
- Prabhu, S. K., Wood, C. H., Miller, D. L., Cernansky, N. P. (1995) "Effect of Nitric Oxide on 1-Pentane Oxidation in the Low and Negative Temperature Coefficient Regimes (600-

800°K)," *Proceedings of Joint Spring Technical Conference of Western, Central States and Mexican Sections of The Combustion Institute*, paper no. 95S-50, pp. 257-262, San Antonio, TX, April 23-26, 1995.

- Reitz, R. D., and Kuo, T.-W. (1989) "Modeling of HC Emissions due to Crevice Flows in Premixed-Charge Engine," SAE paper 892085.
- Ryan III, T. W., and Callahan, T. J., 1988 " Engine and Constant Volume Bomb Studies of Diesel Ignition and Combustion," Soc. Auto. Engrs. Paper no. 881626.
- Tolan, L. E., and Hess, T. D. (1983) "The Pencil Nozzle - Past, Present, and Future," SAE paper 830666.
- Xia, Q. Y., and Flanagan, R. C., 1987 " Ignition Delay - A General Engine/Fuel Model," Soc. Auto. Engrs. Paper no. 870591.
- Zahdeh, A. R., Henein, N. A., and Bryzik, W. (1990) "Diesel Cold Starting: Actual Cycle Analysis under Border-Line Conditions," SAE paper 900441.
- Zahdeh, A. R., and Henein, N. A. (1992) "Diesel Engine Cold Starting: White Smoke," SAE paper 920032.

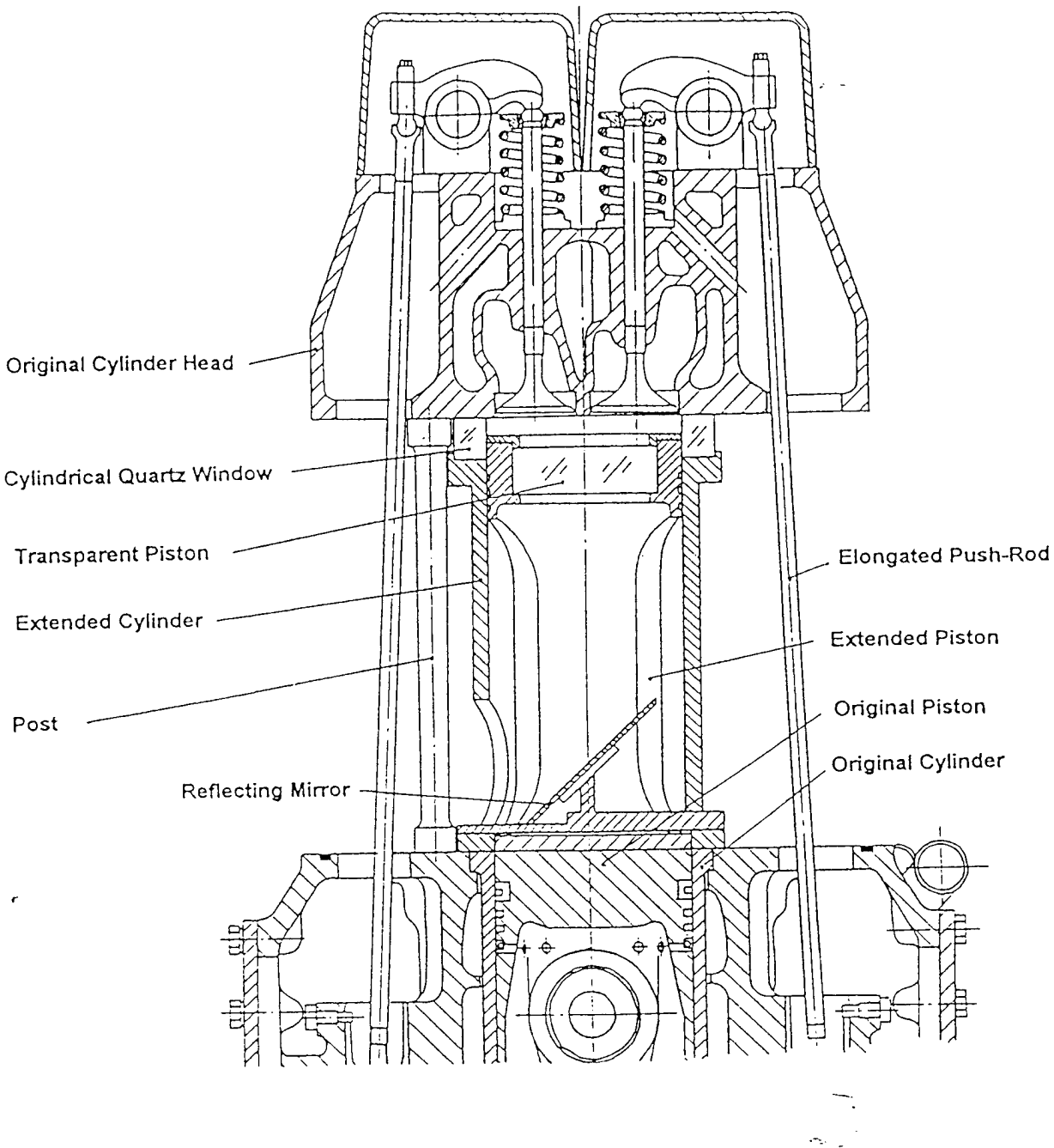

Fig. 1 Schematic of the optical access for AVL engine.

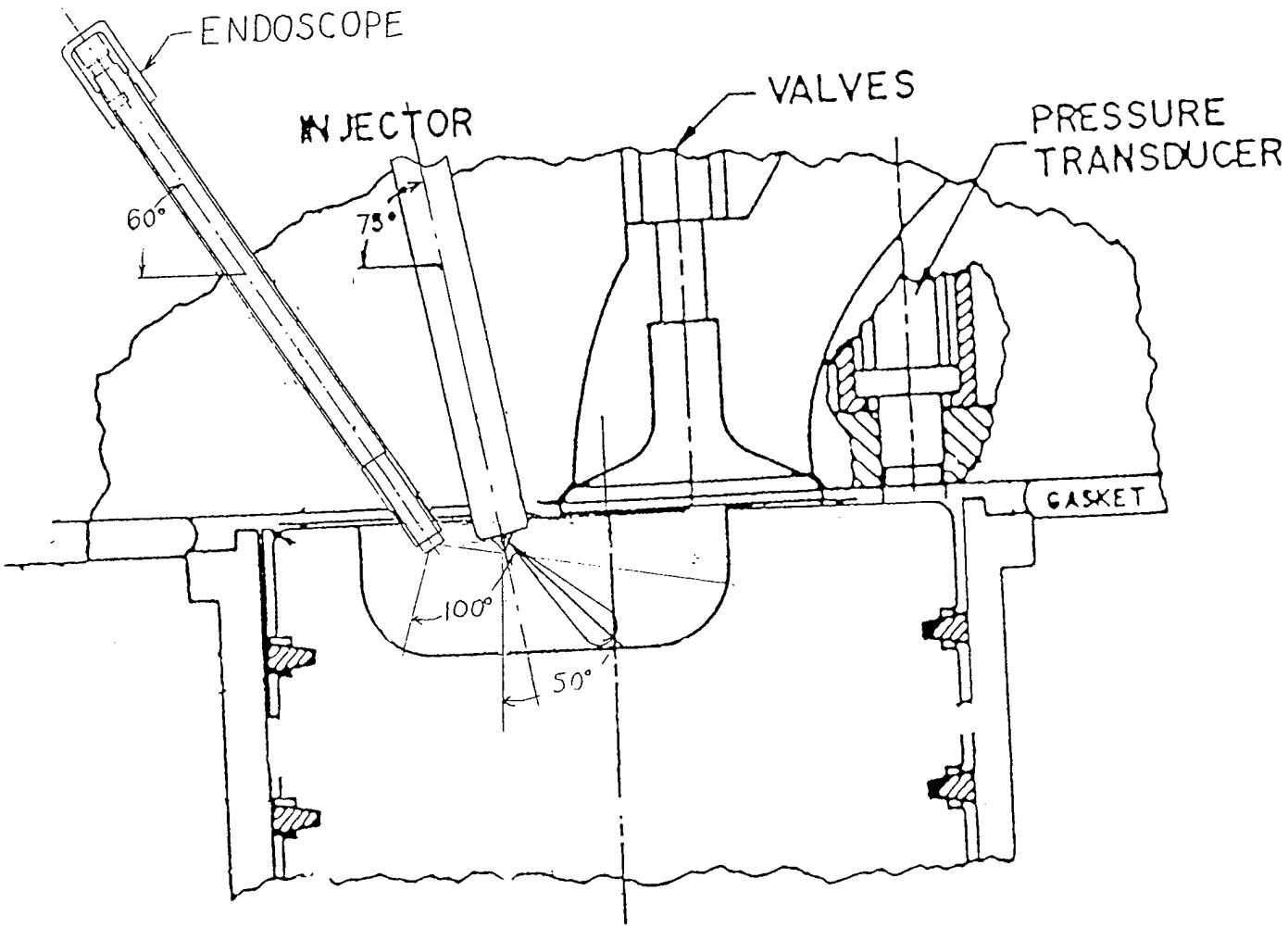

Fig. 2 Schematic of the optical access for LABECO engine.

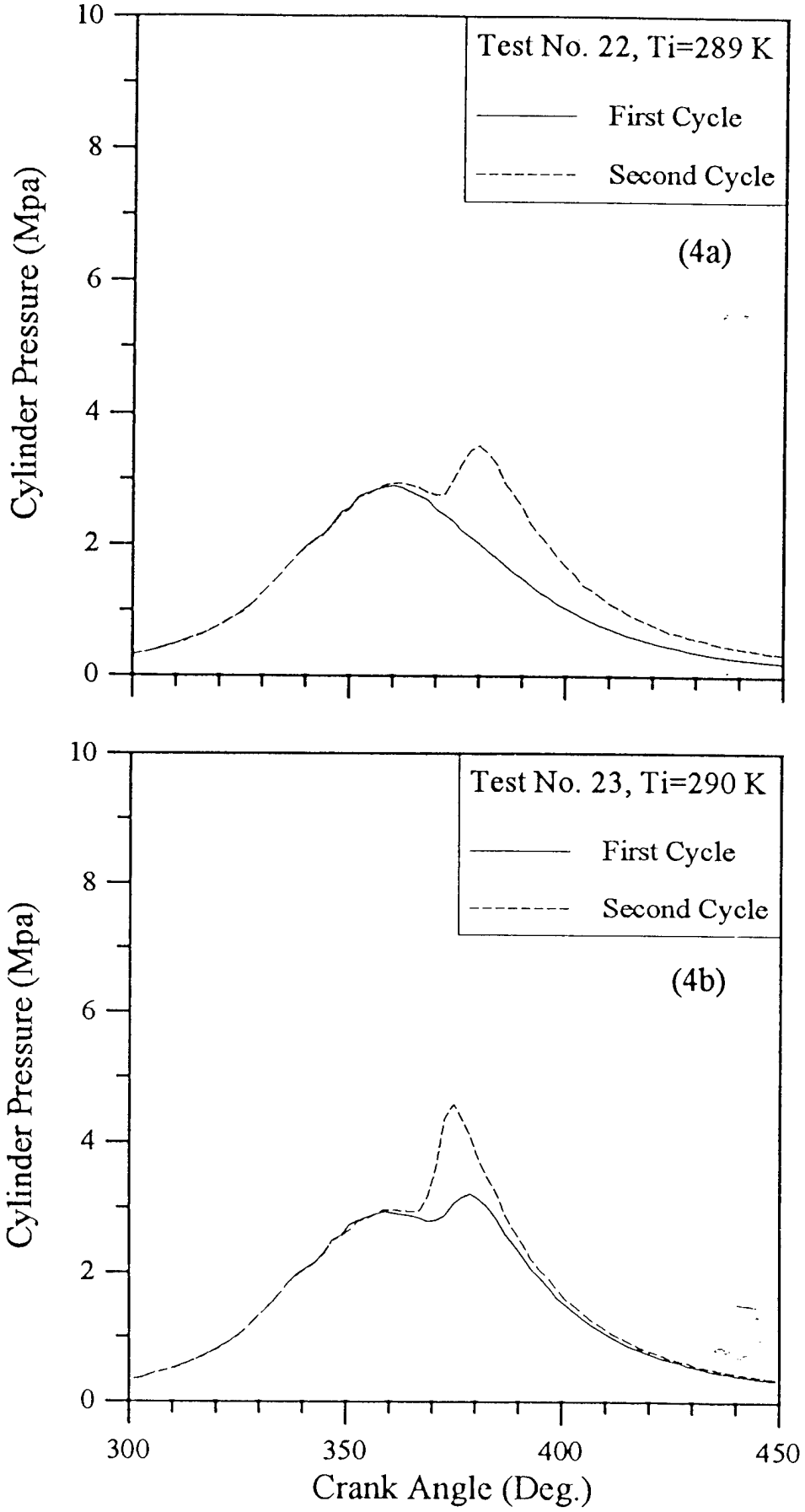

Fig. 4 Cylinder pressure trace of the first two fuel injection cycles for AVL engine: - Effect of temperature and residual gas: a) test No. 22, b) test No. 23.

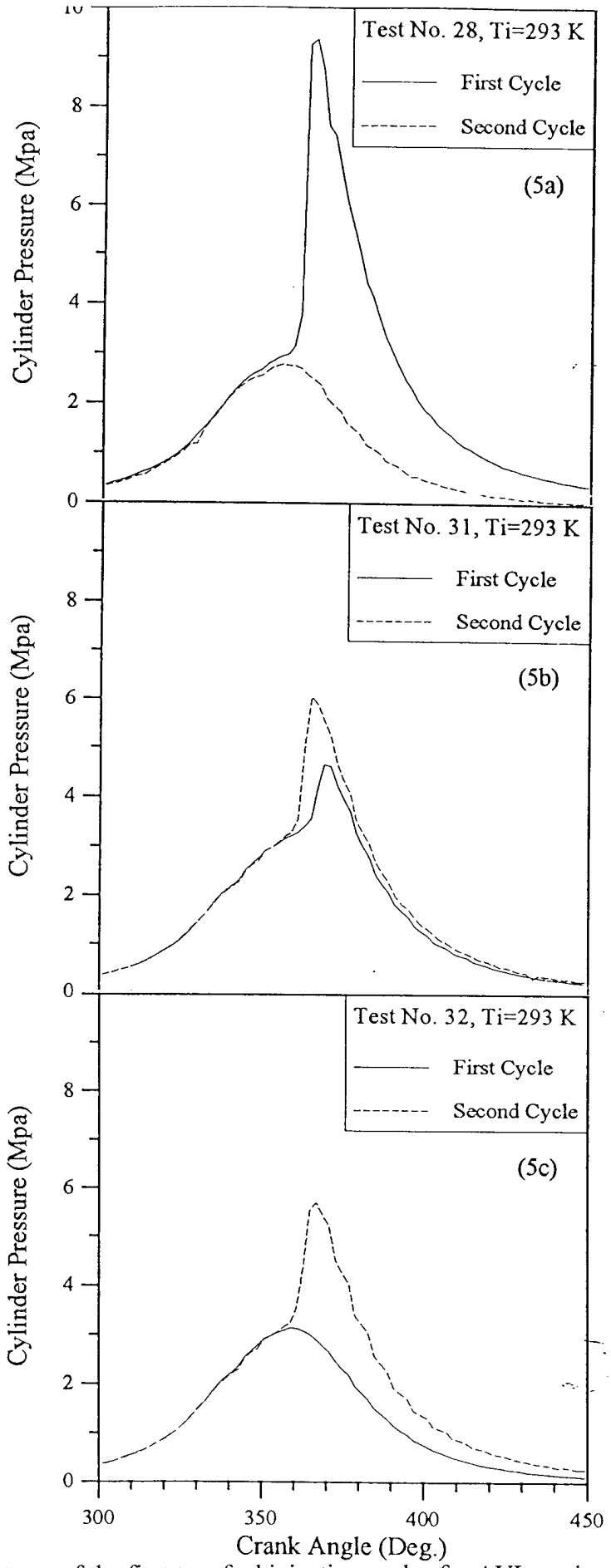

Fig. 5 Cylinder pressure trace of the first two fuel injection cycles for AVL engine: - Effect of amount of fuel injected - a) test No. 28, b) test No. 31, c) test No. 32.

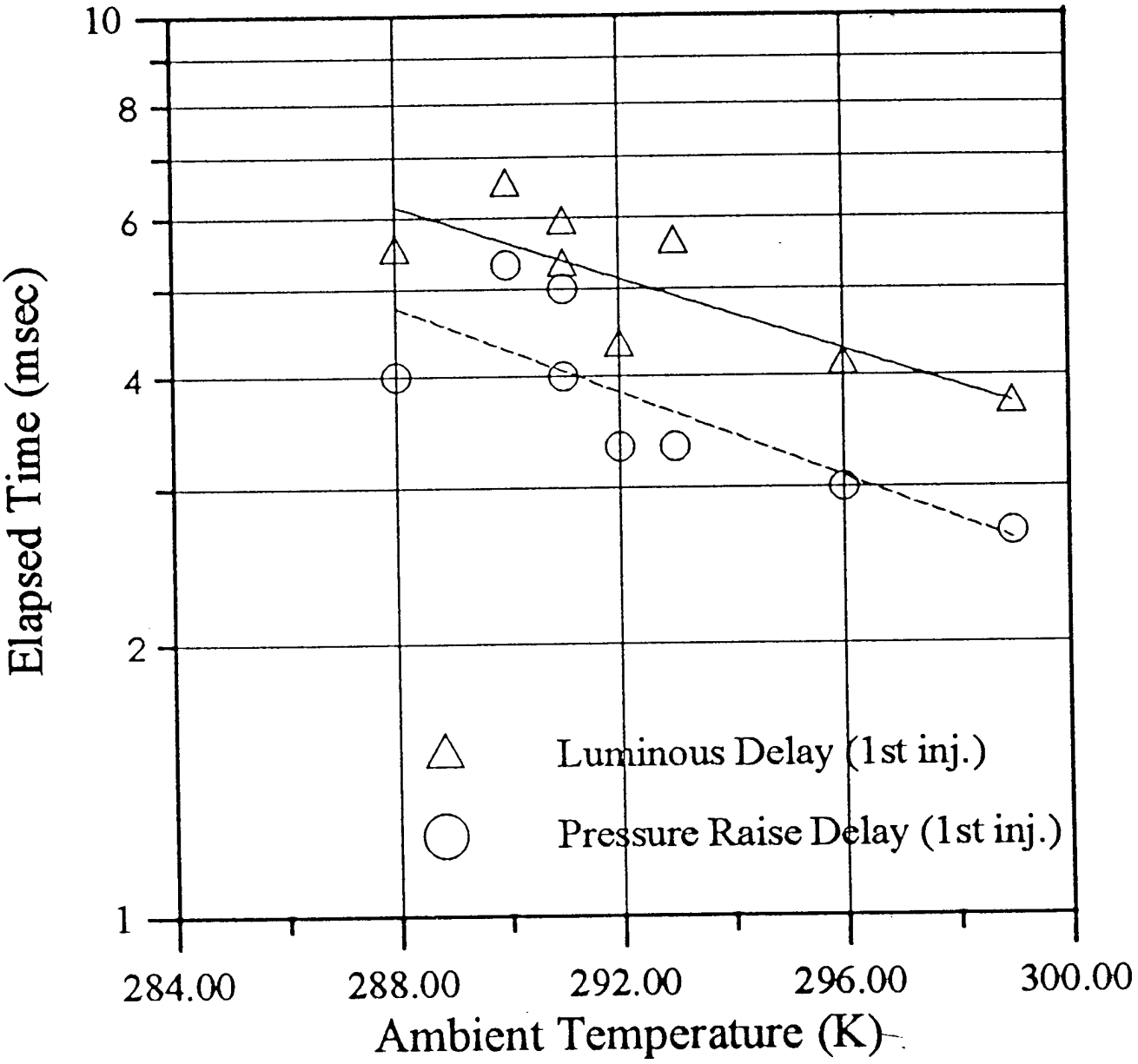

Fig. 6 Time delays based on cylinder pressure rise or observed luminosity for AVL engine at 500 rpm.

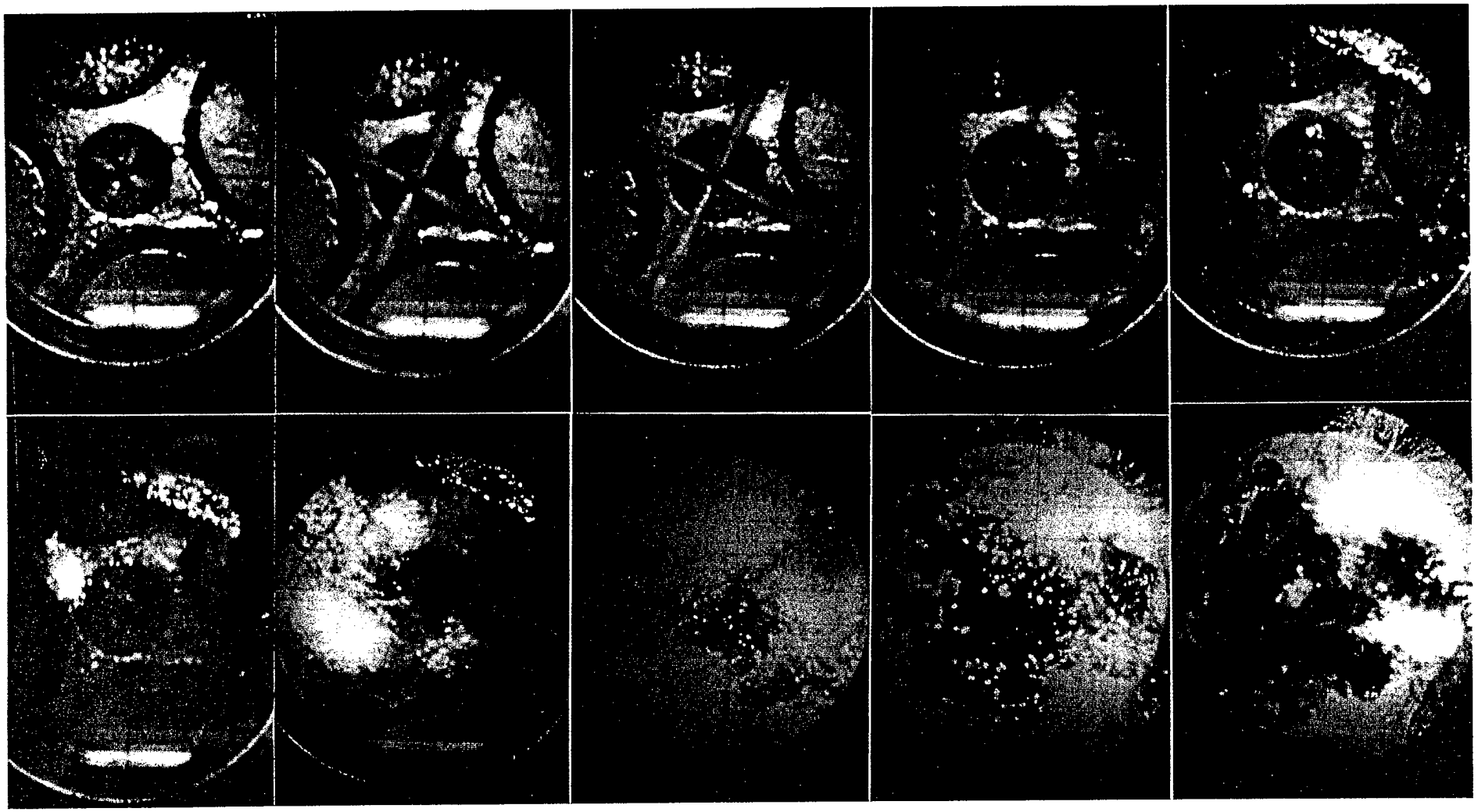

Fig. 7 High-speed movies of a successfully fired cycle for AVL OAE at 291°K ambient temperature. Time between each frame is approximately 0.6 ms.

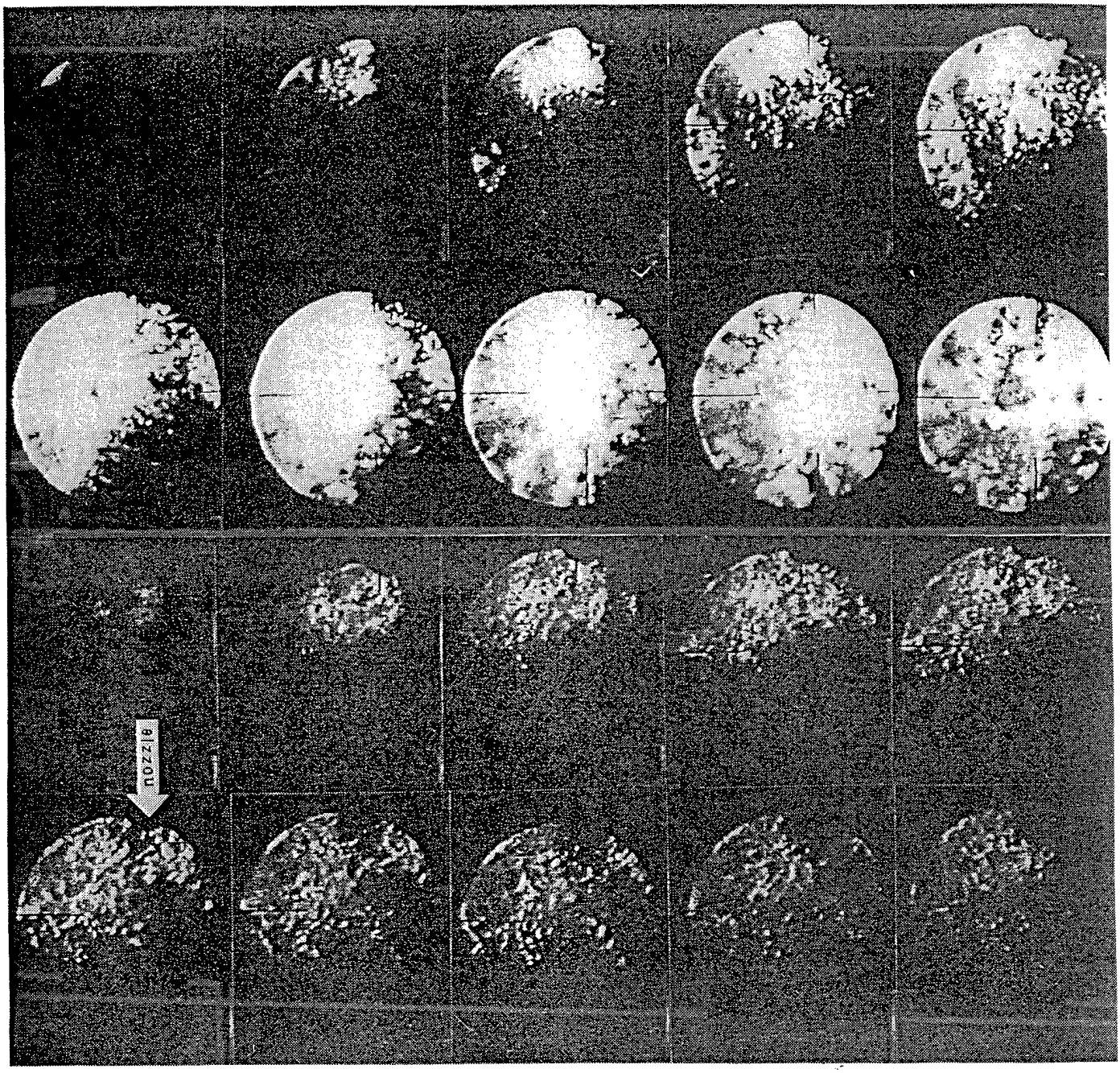

Fig. 8 High-speed movies of the first (top two rows) and second (bottom two rows) cycle of fuel injection for the LABECO engine operated at 283 °K. Time between each frame is approximately 0.67 ms.

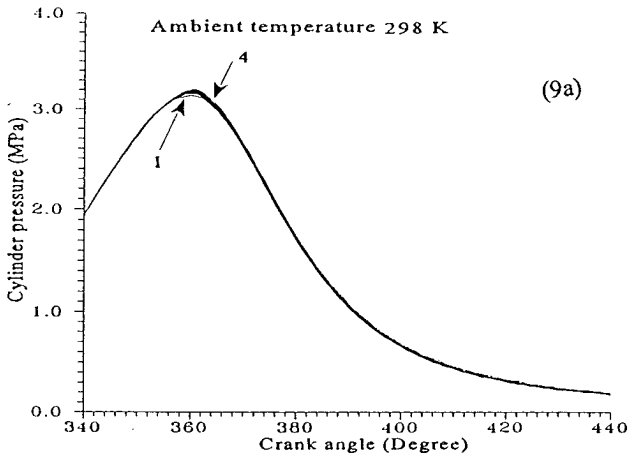

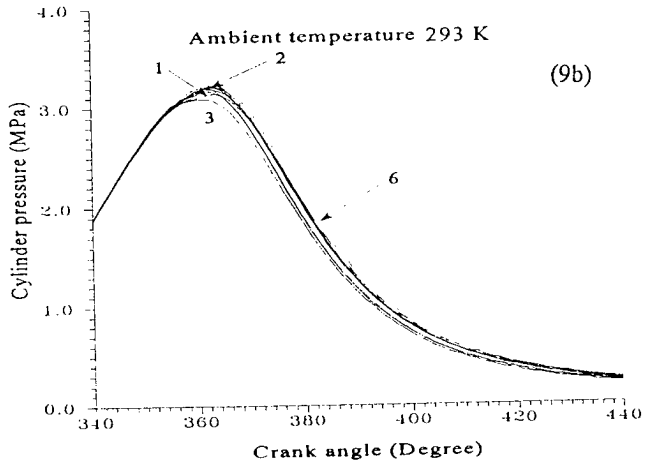

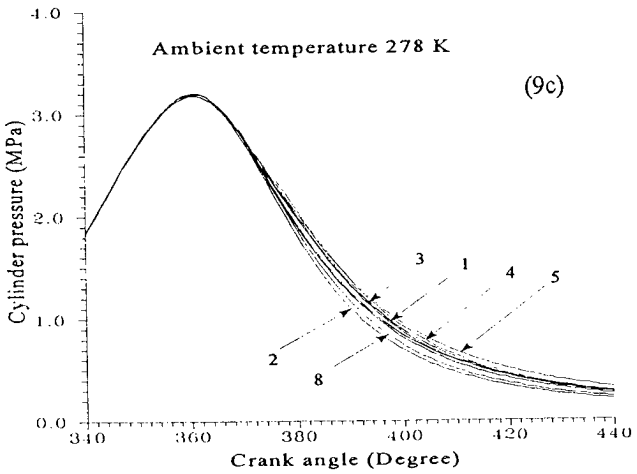

Fig. 9 Cylinder pressure traces of ten consecutive cycles for the LABECO engine operated at a) 298 °K, b) 293 °K, and c) 278 °K.

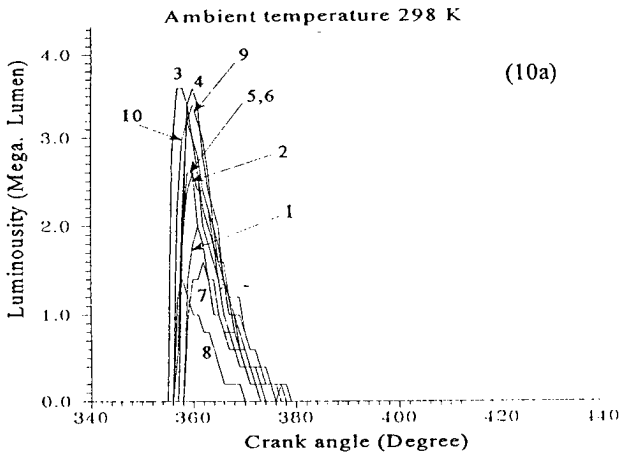

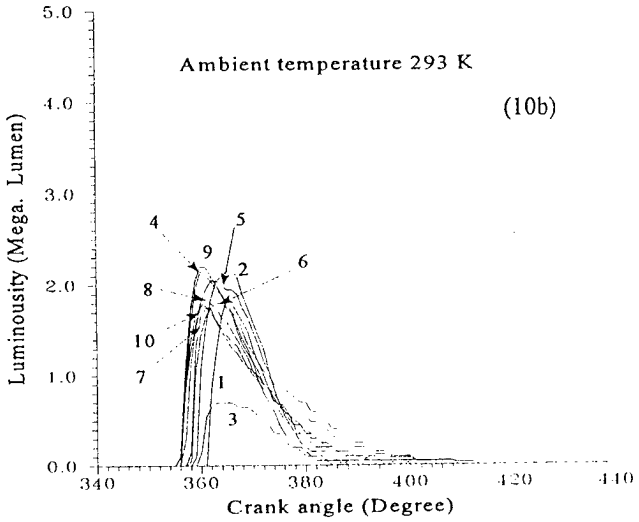

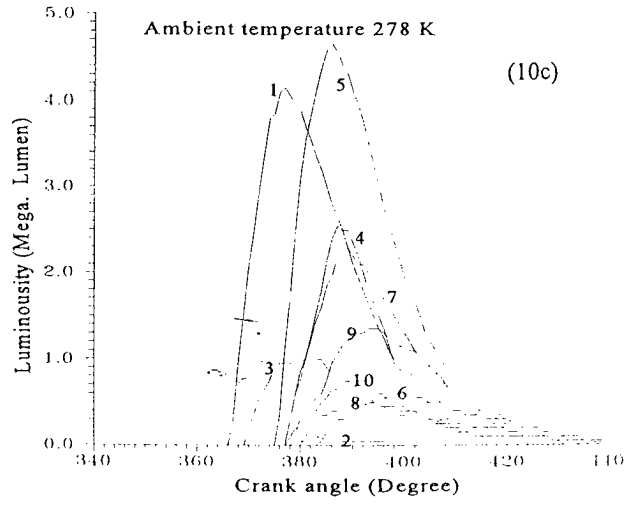

Fig. 10 Luminosity traces of ten consecutive cycles for the LABECO engine operated at a) 298 °K, b) 293 °K, and c) 278 °K.

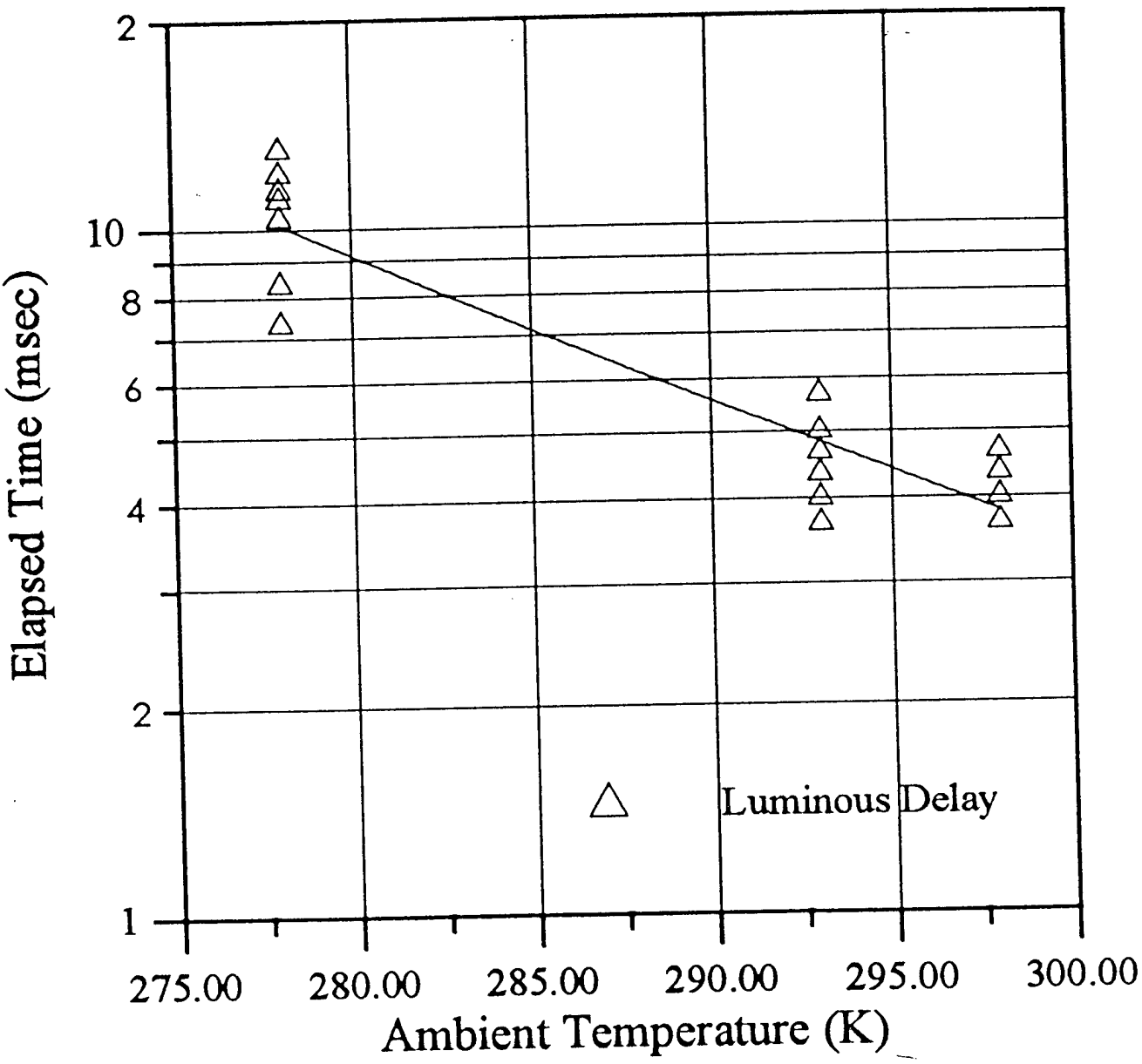

Fig. 11 Time delays based on measured luminosity for LABECO engine at 500 rpm.

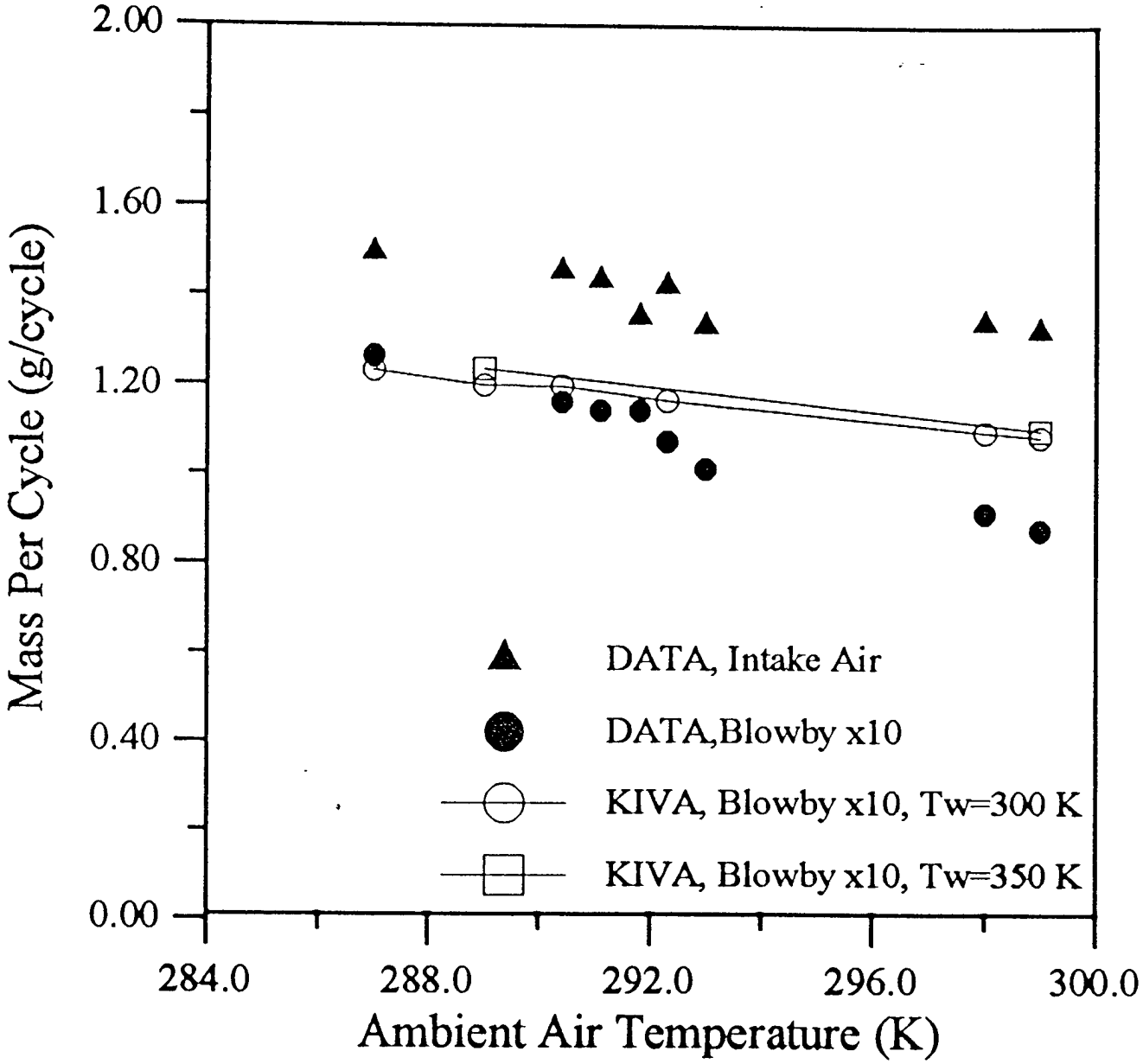

Fig. 12 Intake air and blowby flow rates for AVL engines at 500 rpm.

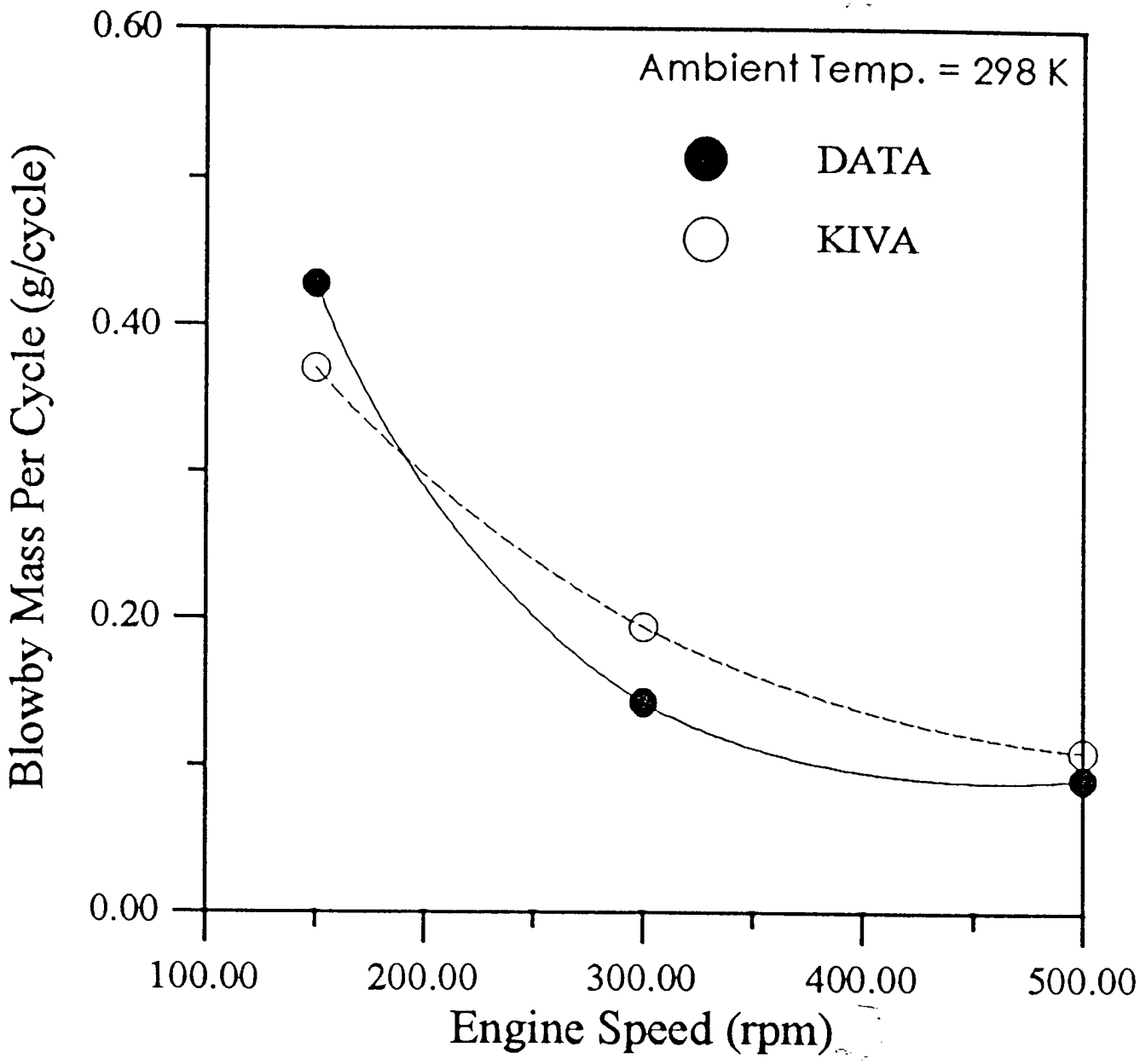

Fig. 13 Blowby flow rates for AVL engines at 298°K.

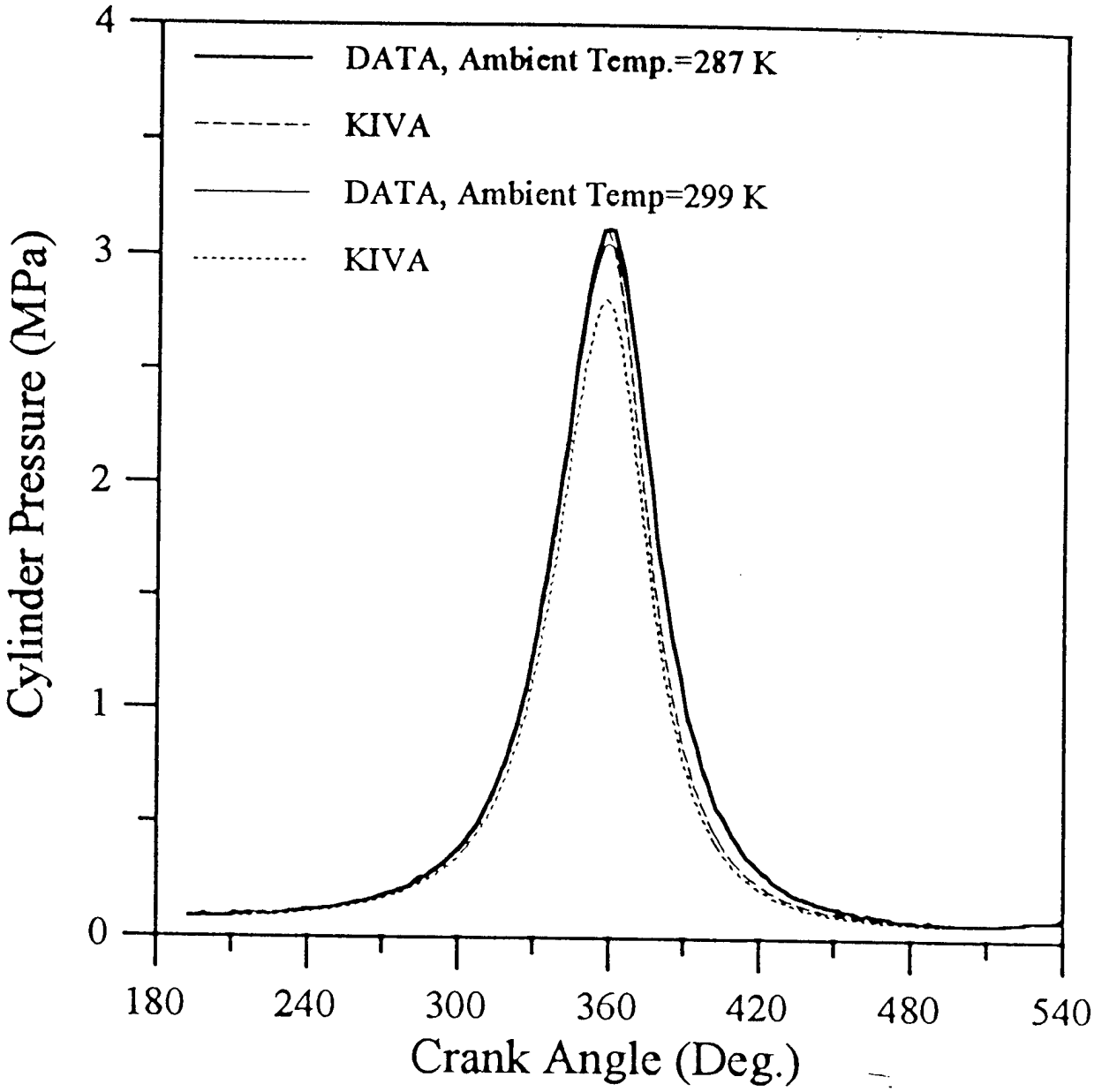

Fig. 14 Predicted and measured cylinder pressures under motoring conditions.

a) Exciplex LIF image of the vapor phase at 0.9 msec after fuel injection

c) Exciplex LIF image of the vapor phase at 1.6 msec after fuel injection

b) Exciplex LIF image of the liquid phase at 0.9 msec after fuel injection

d) Exciplex LIF image of the liquid phase at 1.6 msec after fuel injection

Fig. 15 Filtered LIEF Visualization of Vaporizing Spray

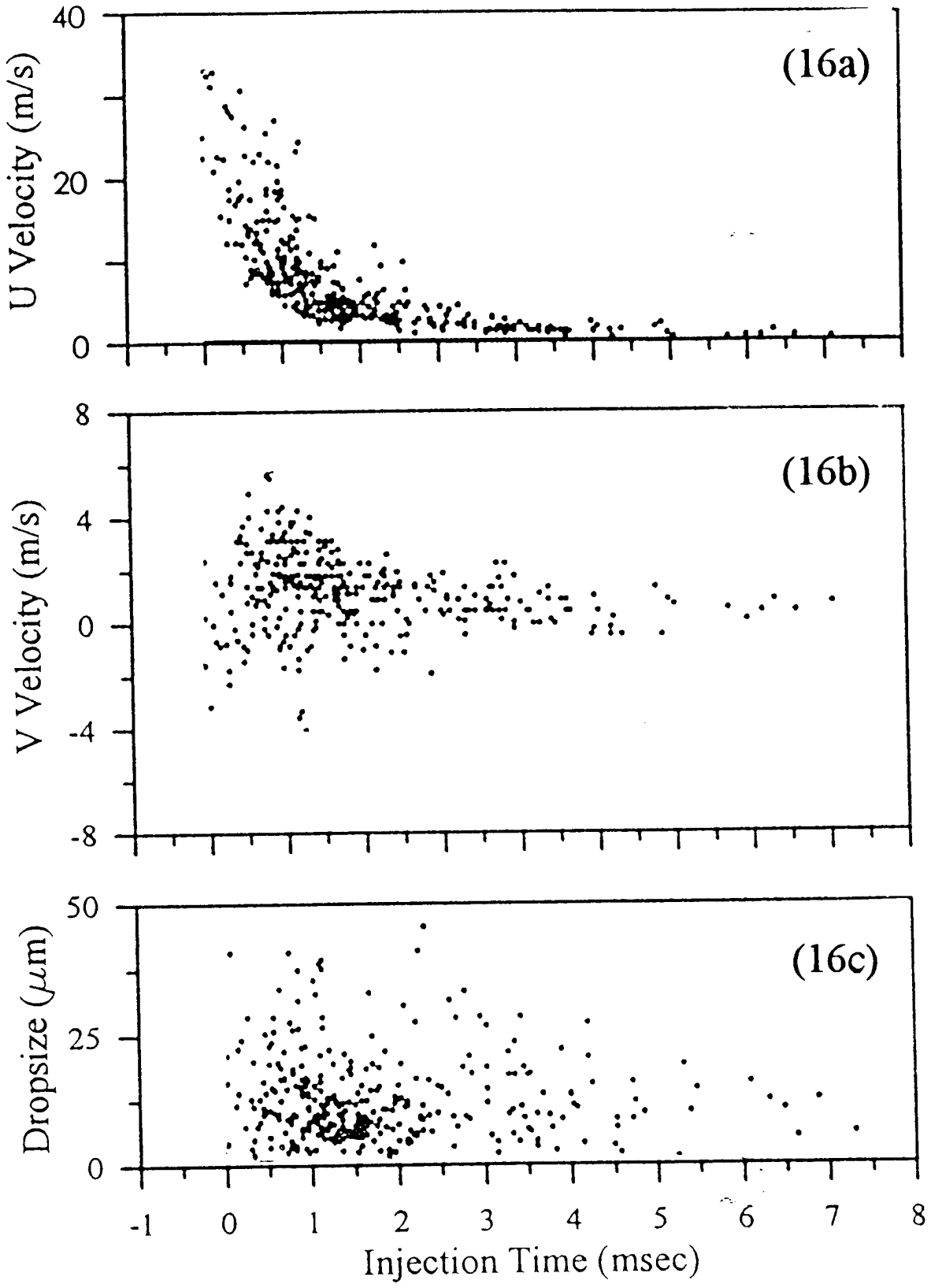

Fig. 16 Time resolved PDPA measurement diesel spray at 30 mm from the injector tip: a) streamwise velocity, b) cross-streamwise velocity, and c) dropsize.

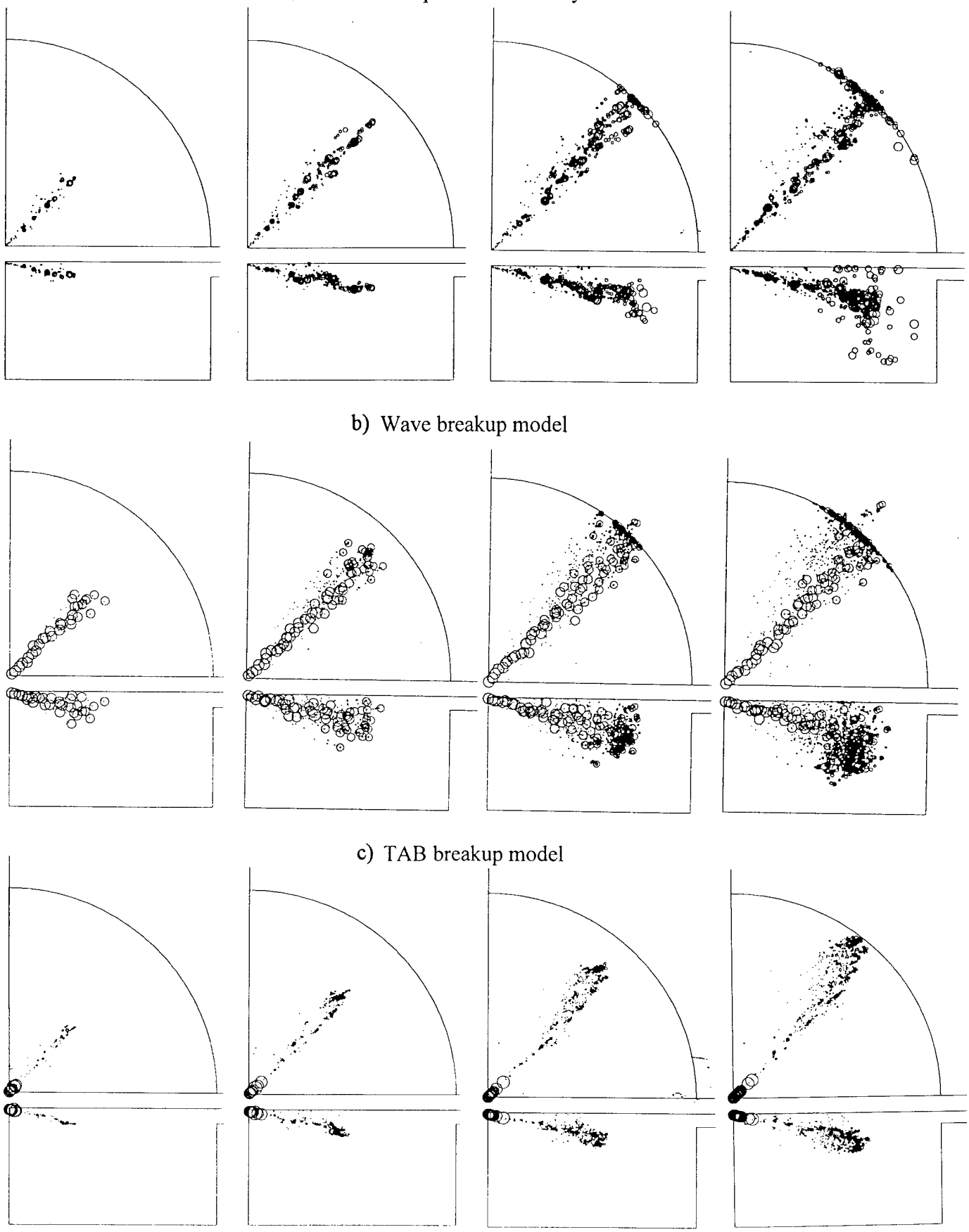

Fig. 17 Spray penetration and dropsize distribution at 1, 2, 3 and 4 degree crankangles after fuel injection

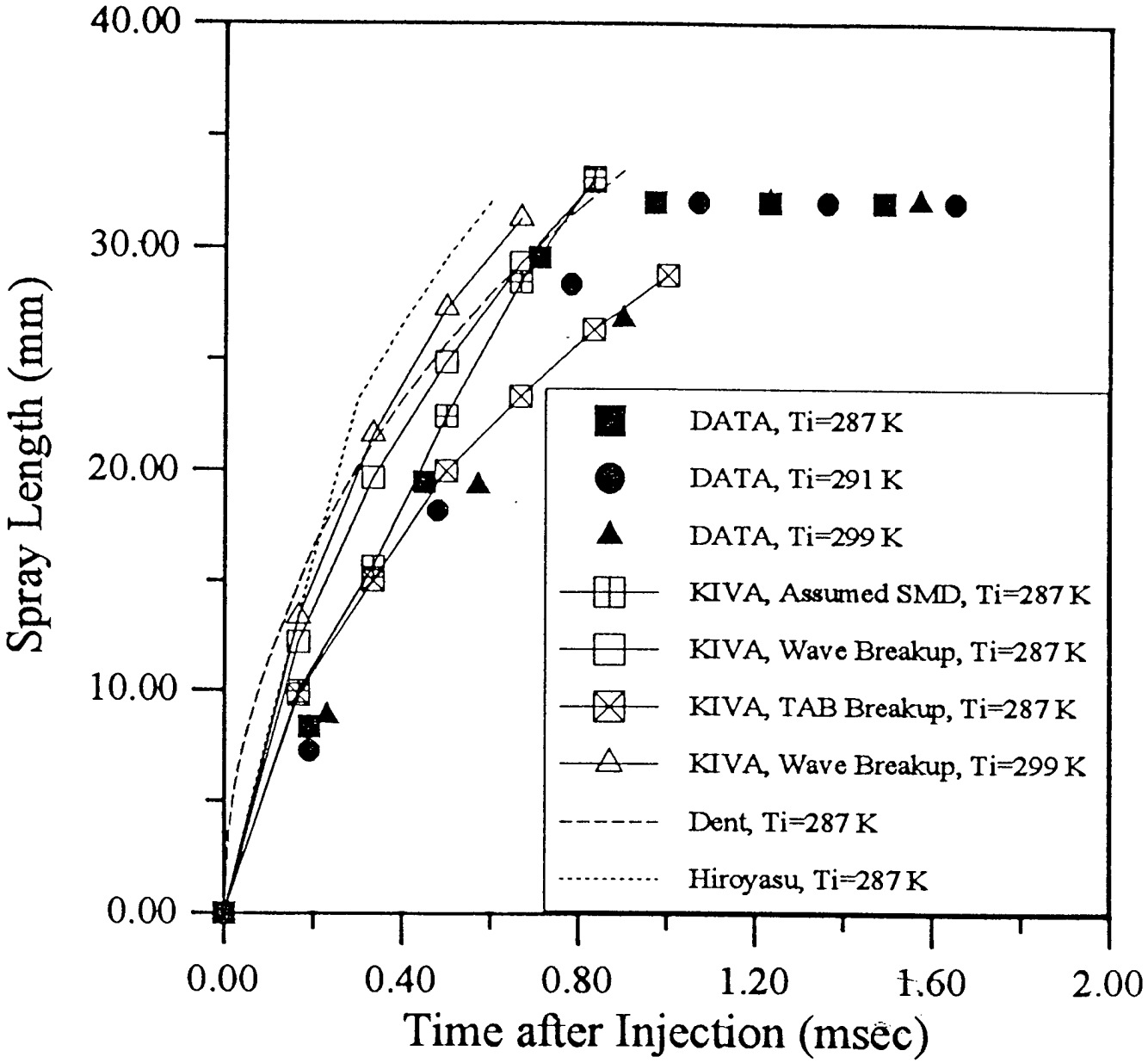

Fig. 18 Comparisons of measured and predicted spray penetrations.

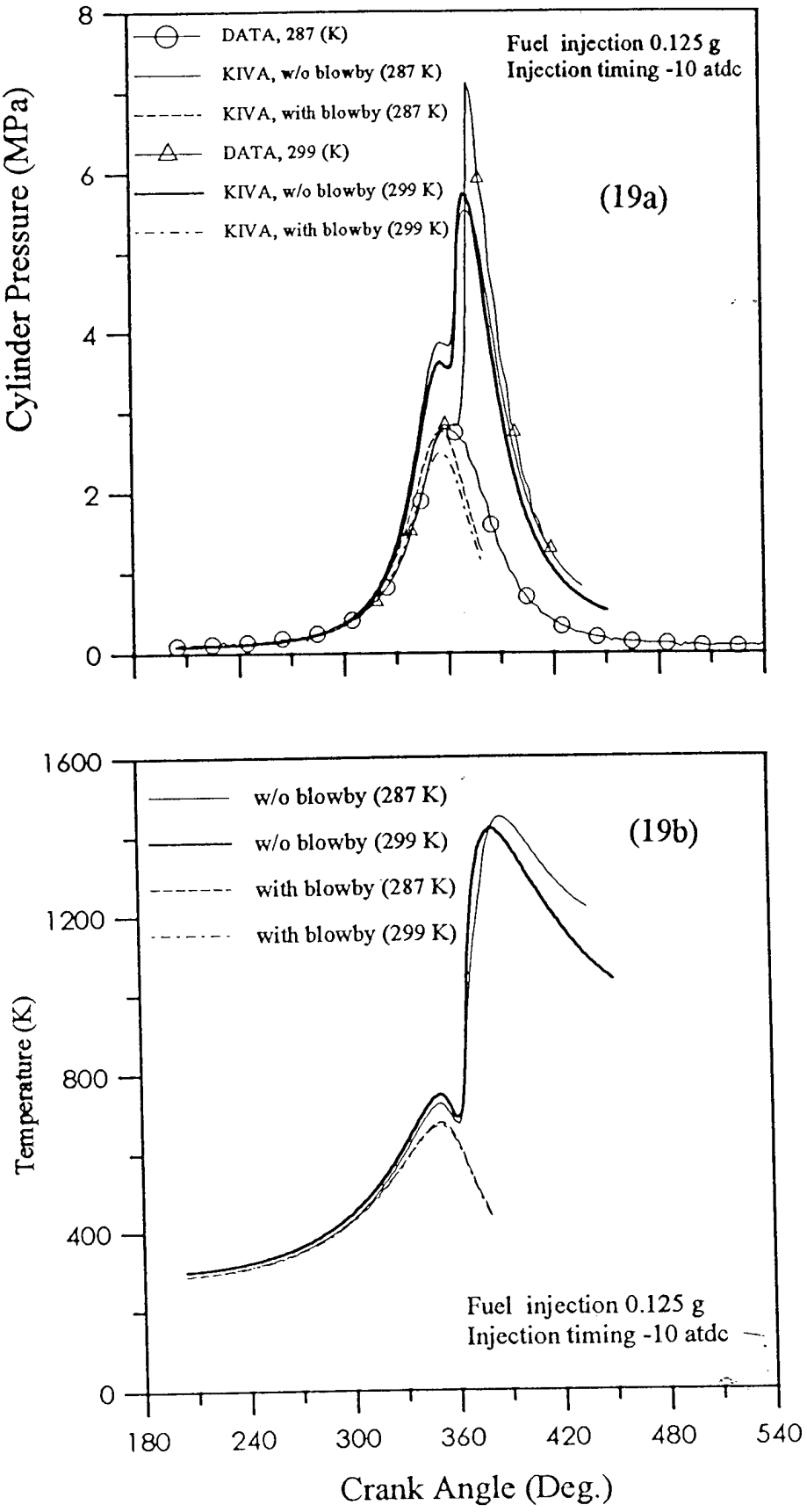

Fig. 19 The effect of intake air temperature on a) cylinder pressures (AVL engine test #2 and 14), and b) the mass-averaged air temperature. Prediction is based on wave breakup model.

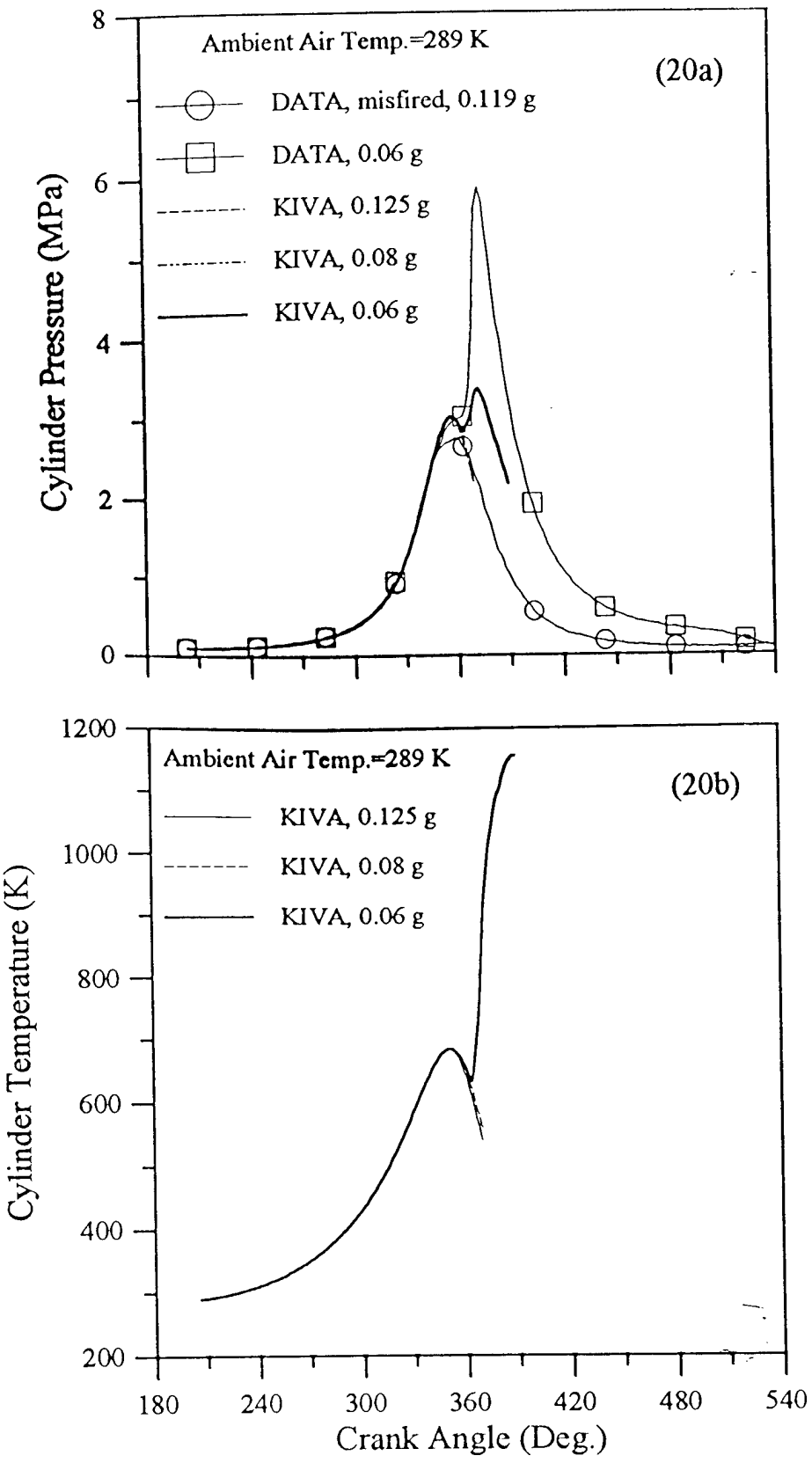

Fig. 20 The effect of the amount of fuel injected on a) the cylinder pressures (AVL engine test # 7 and 17), and b) the mass-averaged air temperature.

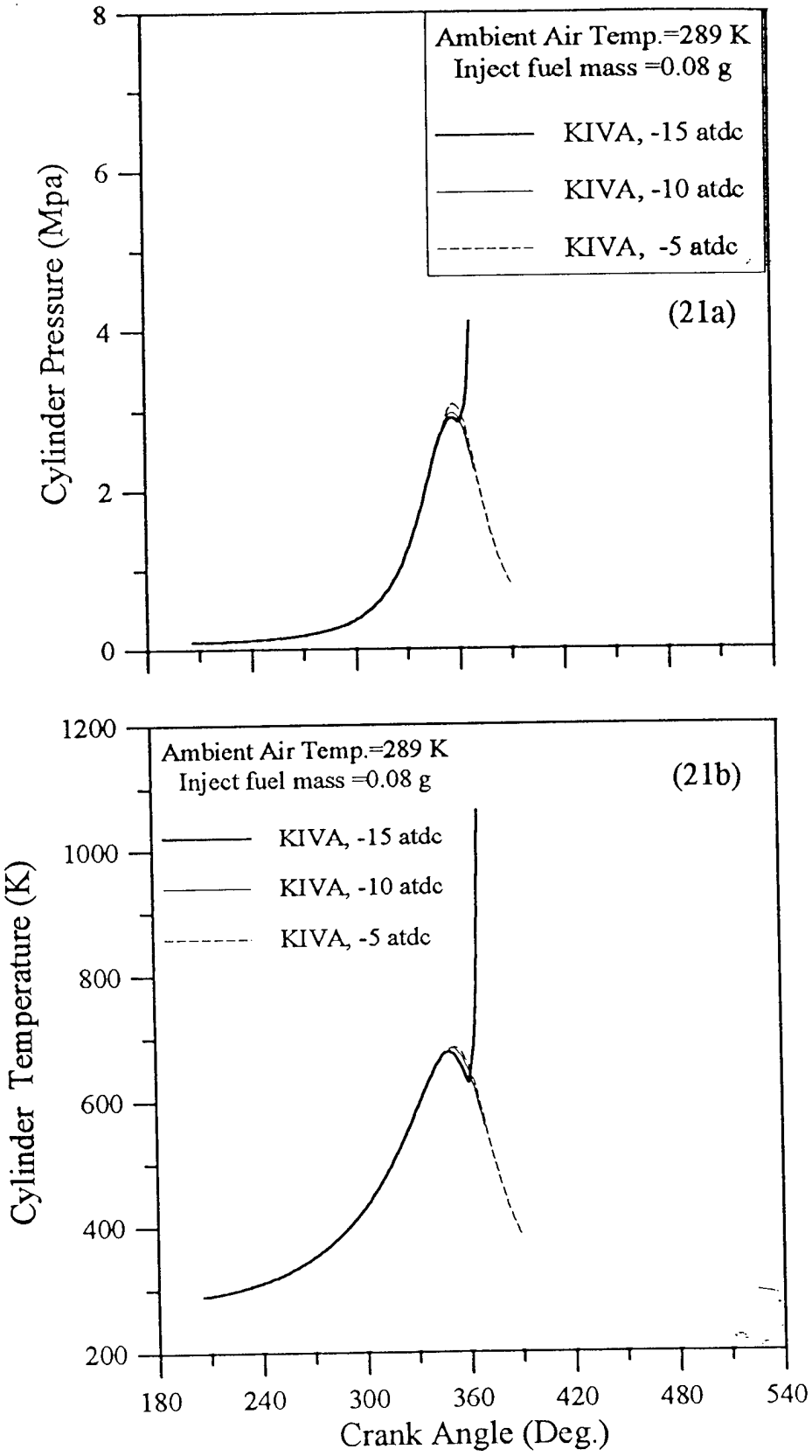

Fig. 21 The effect of fuel injection timing on a) the predicted cylinder pressures, and b) the predicted mass-averaged air temperature.

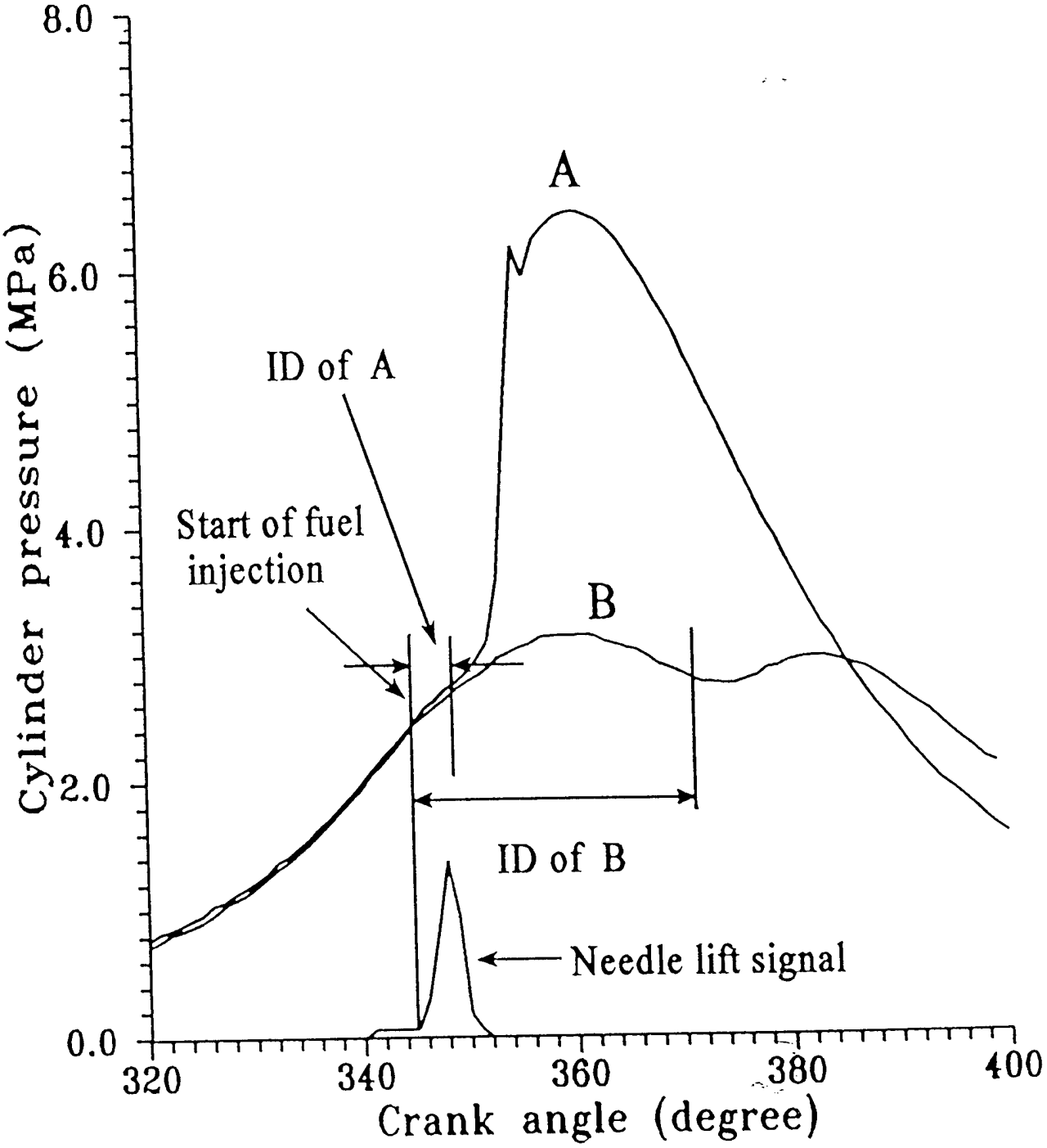

Fig. 22. The definition of ignition delay period in different combustion mode.

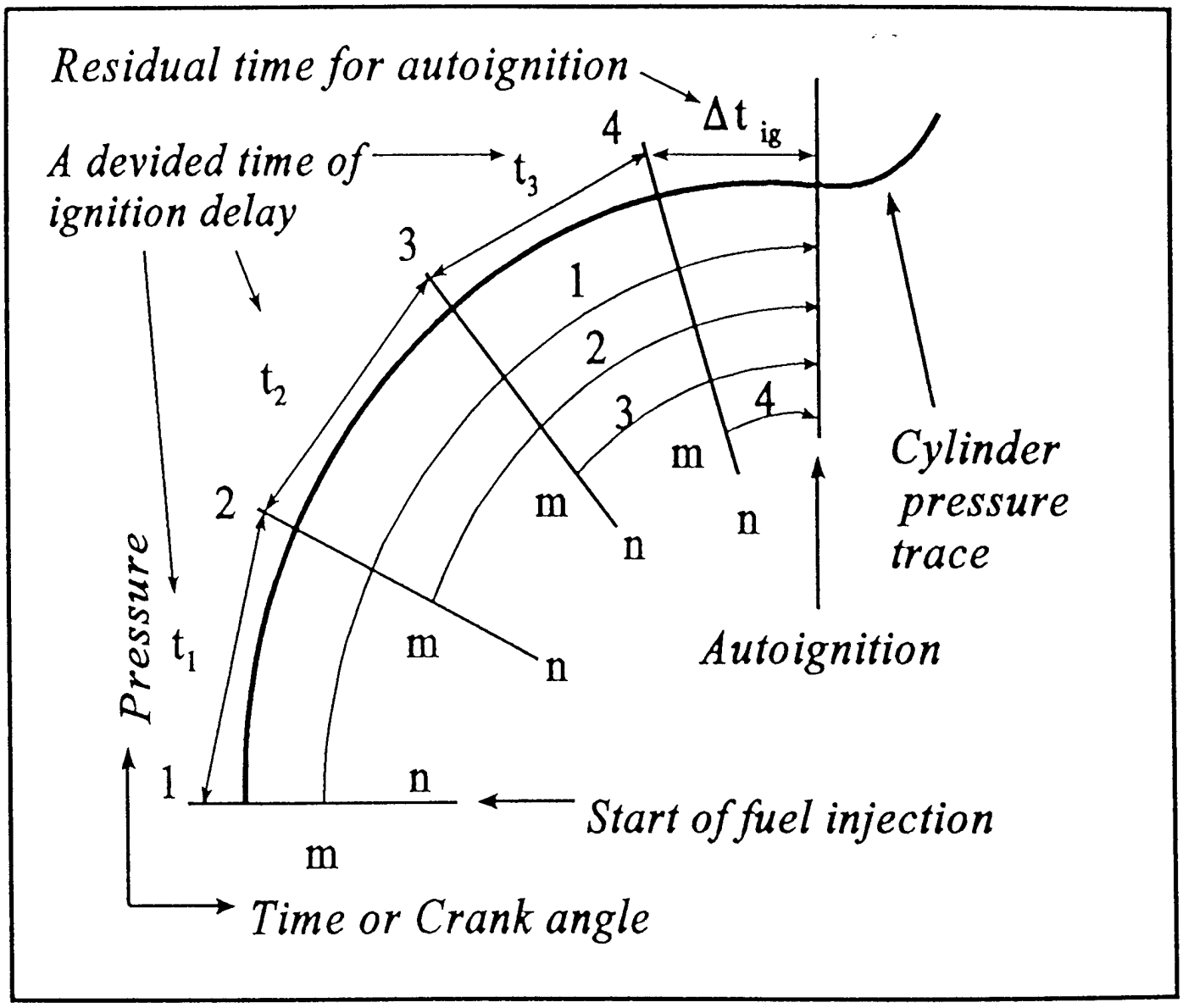

Fig. 23. Pressure -Time diagram for successive elements during ID.

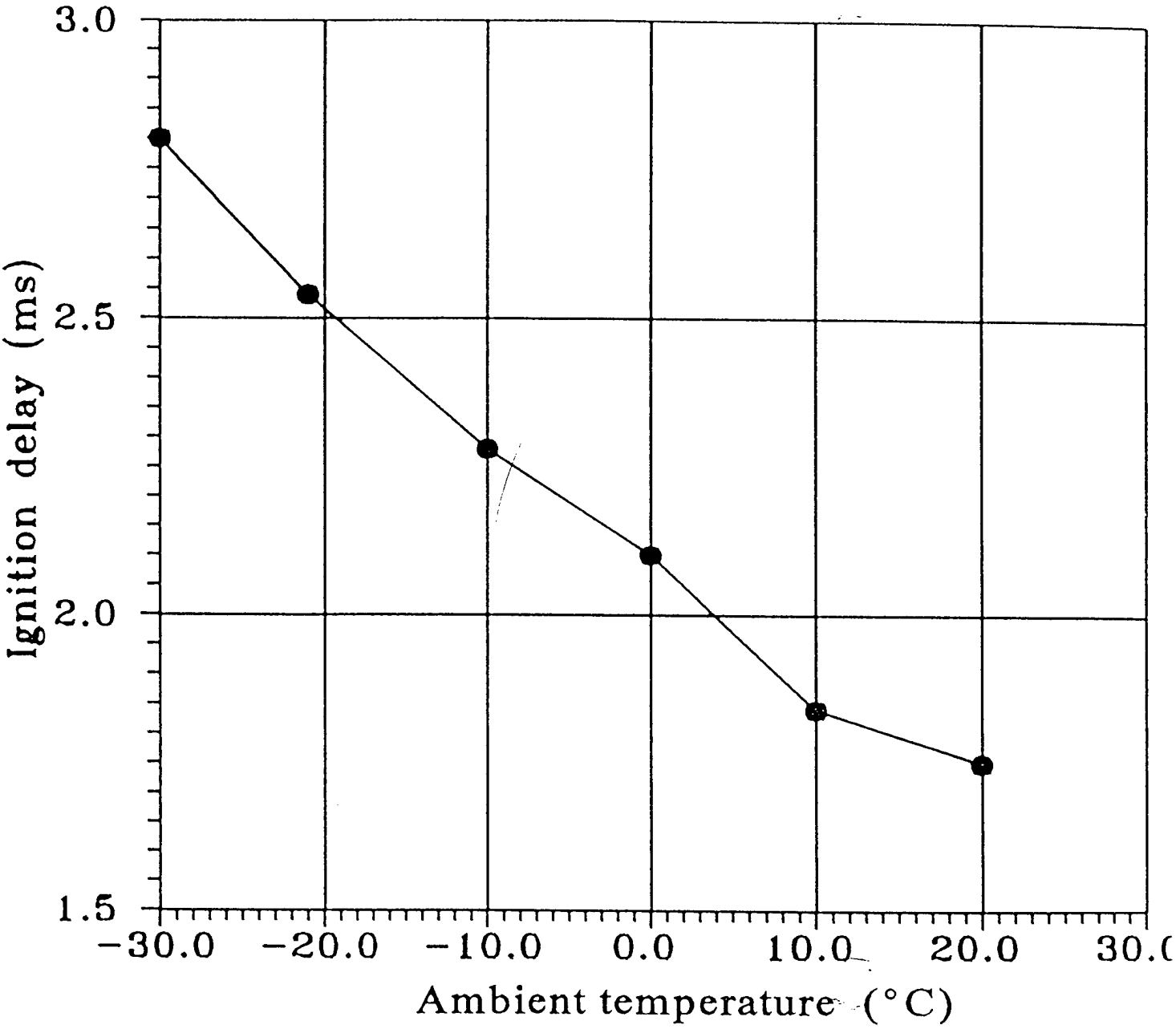

Fig. 24 Experimental data for ignition delay at different ambient temperatures.

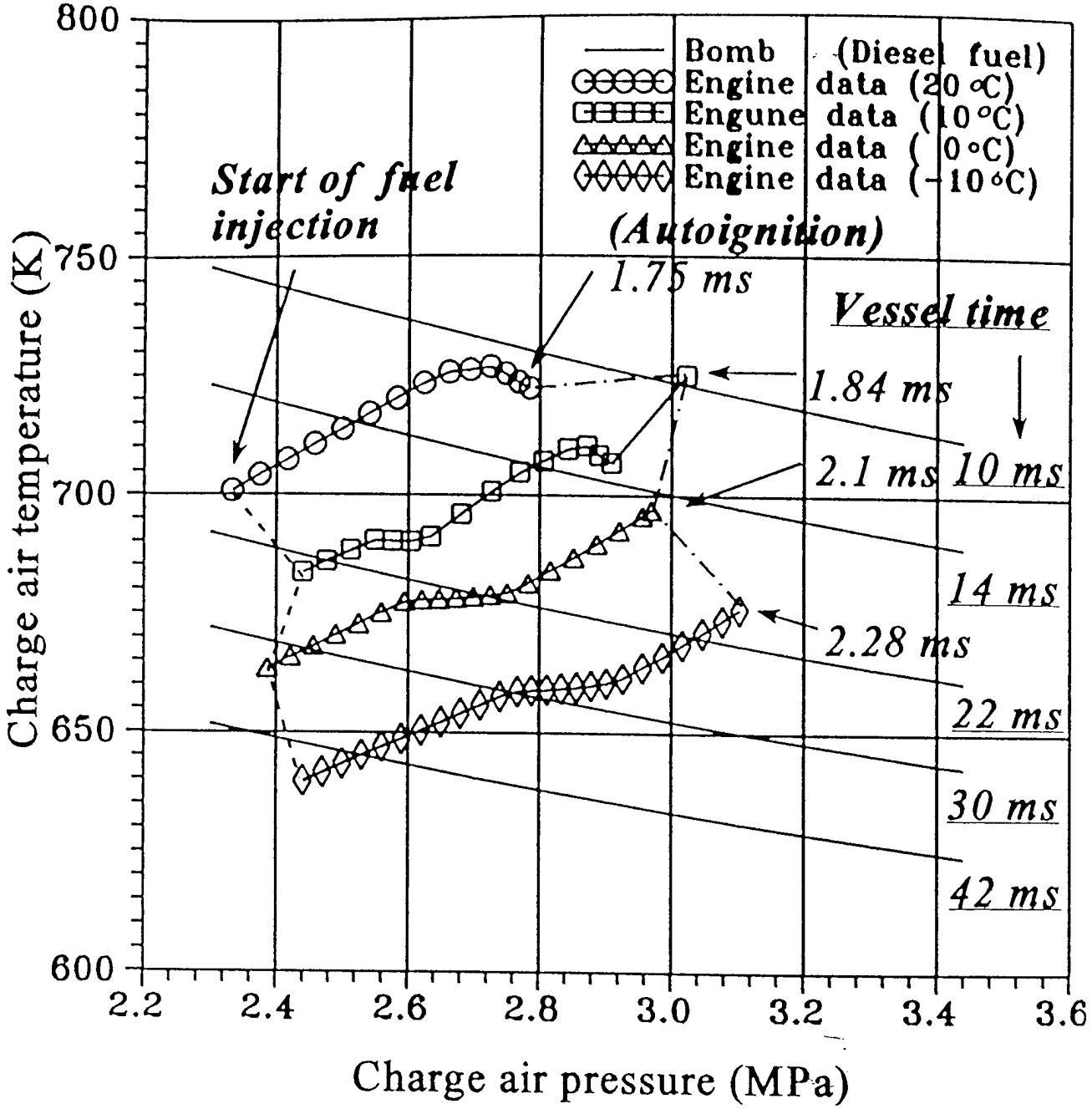

Fig. 25 Ignition delay for vessels and pressure history during ID in engines, at different inlet temperatures.

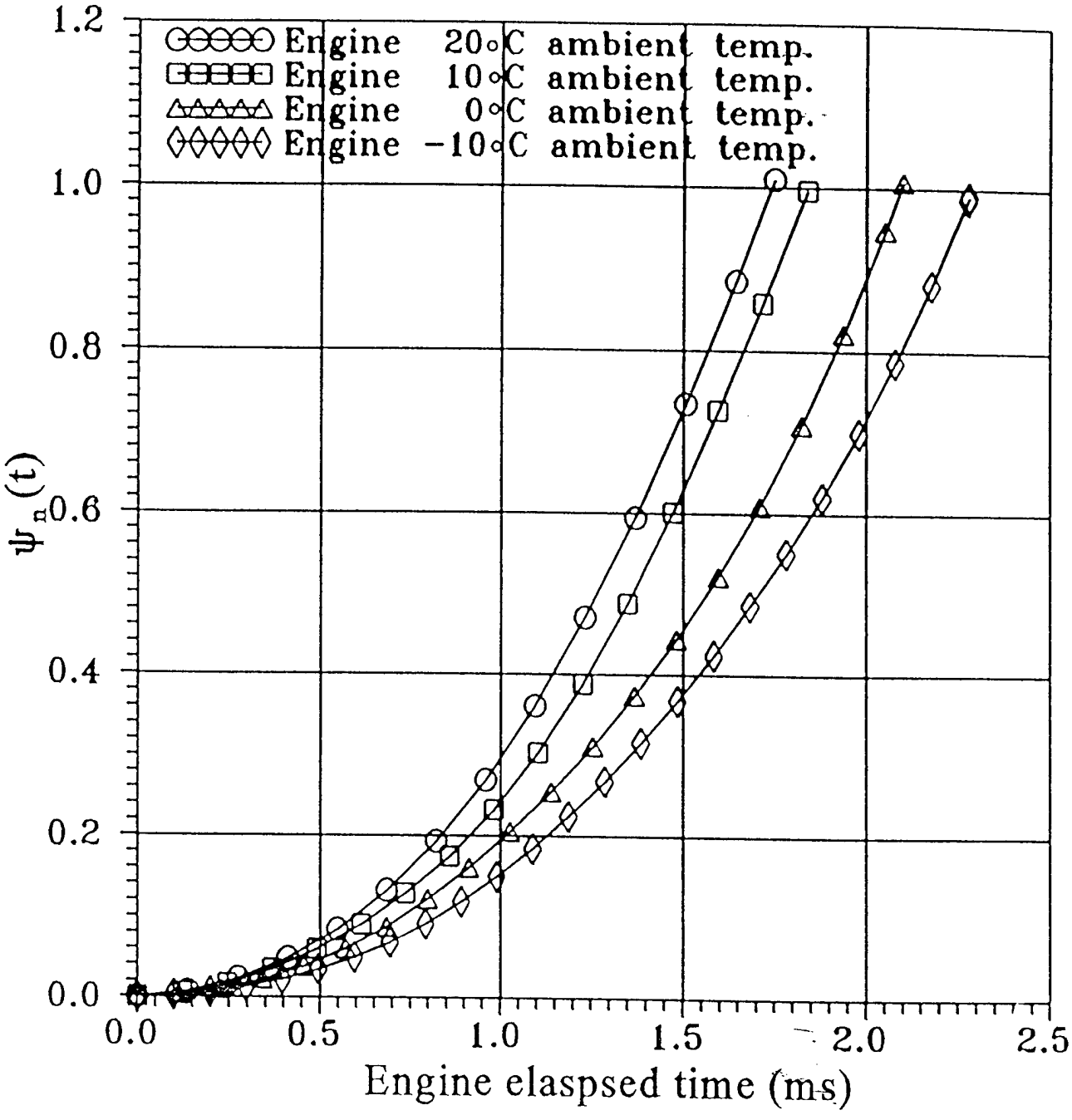

Fig. 26 $\varphi_n(t)$ for different ambient temperatures and for 21 mg per injection.

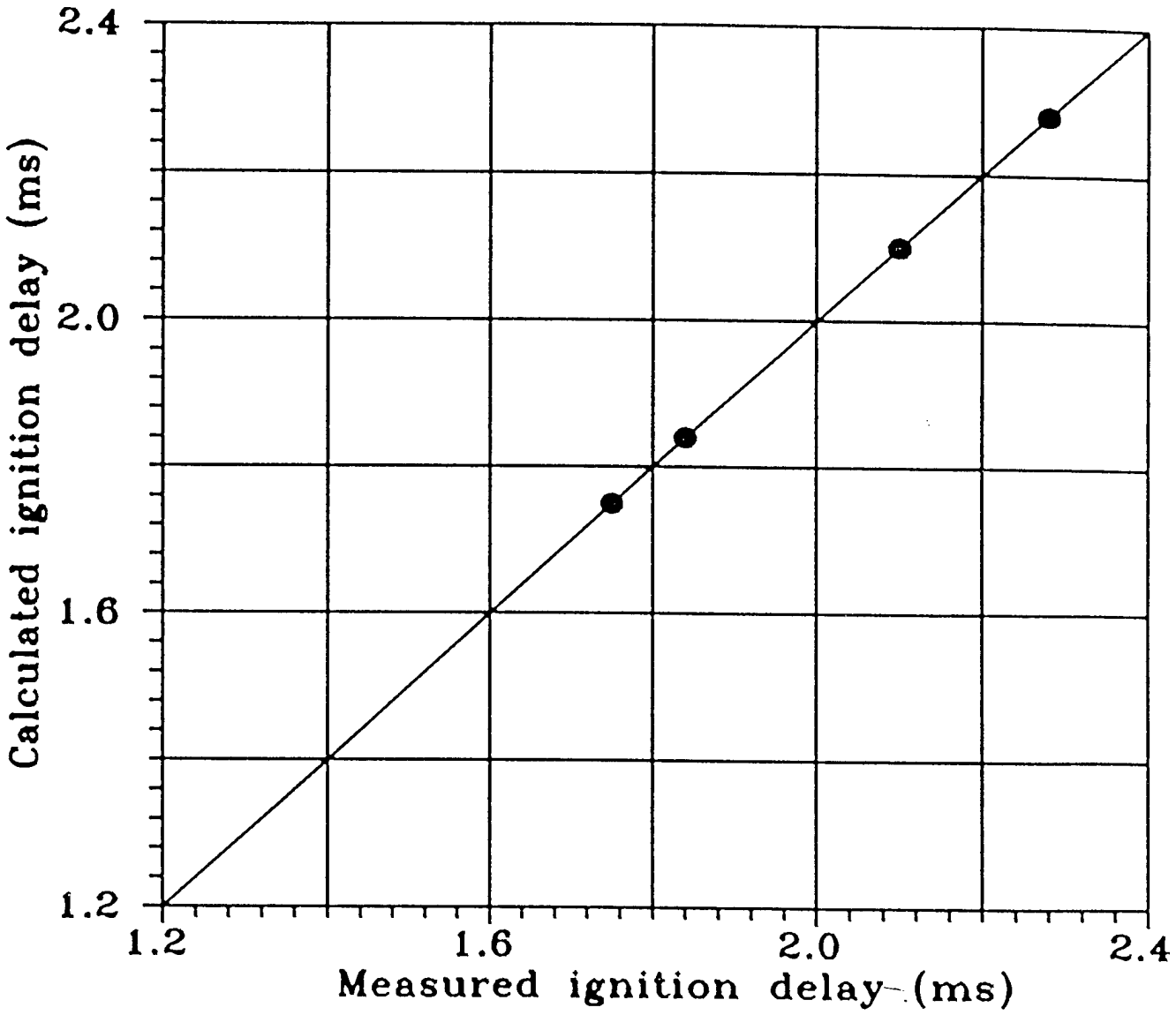

Fig. 27 Comparison of calculated ID period and measured ID period.